

1 A comprehensive non-targeted analysis study of the prenatal 2 exposome

3 Dimitri Panagopoulos Abrahamsson¹, Aolin Wang¹, Ting Jiang², Miaomiao Wang², Adi Siddharth¹, Rachel
4 Morello-Frosch³, June-Soo Park^{1,2}, Marina Sirota^{4,5+} and Tracey J. Woodruff^{1*+}

5

6 ¹ Department of Obstetrics, Gynecology and Reproductive Sciences, Program on Reproductive Health and the
7 Environment, University of California, San Francisco, San Francisco, California, United States.

8 ² California Environmental Protection Agency, Department of Toxic Substances Control, Environmental
9 Chemistry Laboratory, 700 Heinz Ave # 200, Berkeley, CA, 94710, United States.

10 ³ Department of Environmental Science, Policy and Management and School of Public Health, University of
11 California, Berkeley, Berkeley, California, United States.

12 ⁴ Bakar Computational Health Sciences Institute, University of California, San Francisco, California 94158,
13 United States.

14 ⁵ Department of Pediatrics, University of California, San Francisco, California 94158, United States.

15

16

17

18

19

20

21

22 ***Corresponding author: Tracey J. Woodruff** tracey.woodruff@ucsf.edu

23 ⁺These two authors contributed equally to this work.

24 Abstract

25 Recent technological advances in mass spectrometry have enabled us to screen biological samples for a
26 very broad spectrum of chemical compounds allowing us to more comprehensively characterize the human
27 exposome in critical periods of development. The goal of this study was three-fold: 1) to analyze 590 matched
28 maternal and cord blood samples (total 295 pairs) using non-targeted analysis (NTA); 2) examine the differences
29 in chemical abundance between maternal and cord blood samples; and 3) examine the associations between
30 exogenous chemicals and endogenous metabolites. We analyzed all samples with high-resolution mass
31 spectrometry (HRMS) using liquid chromatography – quadrupole time-of-flight mass spectrometry (LC-
32 QTOF/MS), in both positive and negative electrospray ionization modes (ESI+ and ESI-) and in soft ionization
33 (MS) and fragmentation (MS/MS) modes for prioritized features. We confirmed 19 unique compounds with
34 analytical standards, we tentatively identified 73 compounds with MS/MS spectra matching, and we annotated 98
35 compounds using an annotation algorithm. We observed 103 significant associations in maternal and 128 in cord
36 samples between compounds annotated as endogenous and compounds annotated as exogenous. An example of
37 these relationships was an association between 3 poly and perfluoroalkyl substances (PFAS) and endogenous fatty
38 acids in both the maternal and cord samples indicating potential interactions between PFAS and fatty acid
39 regulating proteins.

40

41

42

43

44

45

46

47

48 1. Introduction

49 The exposome describes the sum of all our exposures, both external and internal, throughout our lives
50 from conception and onwards.^{1,2} Humans are exposed to multiple and variable environmental contaminants in
51 both the indoor and outdoor environments through inhalation, ingestion, and dermal absorption. Environmental
52 exposures have been shown to play an important role in the development of human disease along with exposures
53 to endogenous chemicals and genetic predisposition.^{1,2}

54 Exposures to environmental contaminants during pregnancy are of critical importance due to the
55 increased risk for adverse health outcomes that occur during periods of critical and unique susceptibility to
56 biological perturbations, which can increase the risk of both maternal and child adverse health outcomes³⁻⁶.
57 Prenatal exposures to industrial chemicals have been shown to increase the risk of complications during
58 pregnancy, such as preterm birth, pregnancy-related hypertension, adverse birth outcomes, developmental and
59 neurodevelopmental problems during infancy, and disease during adulthood.³⁻⁶

60 Approximately 40,000 chemicals are registered on the inventory of the Toxic Substances Control Act
61 (TSCA) as actively used chemicals in the U.S.^{7,8} This number does not include chemicals that are regulated by
62 other U.S. statutes, such as pesticides, foods and food additives, drugs, cosmetics, tobacco and tobacco products,
63 and nuclear materials and munitions.^{7,8} The actual number of all chemicals used in the U.S. remains unclear but
64 exceeds 40,000.

65 Conventional biomonitoring and human exposure research rely on targeted analytical chemistry
66 techniques, in which one measures chemicals selected prior to the analysis. Up to now, with targeted techniques,
67 only about 350 chemicals are biomonitored regularly via U.S. NHANES, constituting less than 1% of the
68 chemicals used in the US. This limited number of measured targeted chemicals hinders our understanding of
69 human exposure to chemicals and how they may impact human health. Considering the large number of
70 chemicals that are not covered by these approaches, there is a need to develop more high-throughput approaches
71 that cover a broader spectrum of human exposure to environmental contaminants.⁹

72 Recent advances in high-resolution mass spectrometry have brought non-targeted analysis (NTA) and
73 suspect screening to the forefront of analytical chemistry. Non-targeted analysis techniques offer the possibility to
74 screen biological and environmental samples for a very broad spectrum of chemicals that would previously
75 remain undetected with conventional targeted analytical techniques. Such high-throughput analytical techniques
76 enable a more holistic characterization of the exposome incorporating both internal (endogenous) and external
77 (exogenous) exposures. Previous non-targeted and suspect screening studies¹⁰⁻¹⁵ have demonstrated the value of
78 NTA as an important screening tool for compound discovery in environmental applications. The compounds
79 discovered through NTA can then inform more traditional targeted analytical approaches to further evaluate
80 chemicals of interest with more stringent quality assurances that include further examination with analytical
81 standards and quantification.

82 Our work builds upon previous NTA and suspect screening studies^{11-13,16-18} of other scientific groups that
83 have laid the groundwork for further analysis and have inspired further exploration. In our study, we developed an
84 enhanced NTA workflow to screen human biological samples for a broad spectrum of chemicals that can be
85 identified or tentatively identified, and then applied this approach to study exogenous and endogenous chemical
86 exposures in a large racially and socioeconomically diverse population of pregnant women. The novelty of our
87 work lies primarily in the analysis of a large cohort of maternal and cord blood samples and in the selection and
88 combination of computational tools for the analysis and interpretation of non-targeted analysis data. Our study
89 aims to explore the computational, analytical and environmental chemistry aspects of non-targeted analysis and
90 explore the human exposome during pregnancy through the lens of chemistry.

91 The goal of this study was three-fold: 1) to analyze 590 matched maternal and cord blood samples (total
92 295 matched pairs) using NTA to characterize the maternal/fetal exposome; 2) examine the differences in
93 chemical feature enrichment between maternal and cord blood samples; and 3) examine the associations between
94 exogenous chemicals and endogenous metabolites in an attempt to understand the interplay between the
95 exposome and the metabolome.

96 2. Materials and Methods

97 2.1 Study population

98 The study population consisted of 295 pregnant women recruited during the Chemicals in Our Bodies
99 (CIOB) study (Table 1) at the University of California, San Francisco (UCSF). The CIOB study consists of about
100 700 (as of the time of this publication) English or Spanish-speaking pregnant women, aged 18 to 40 years old and
101 with singleton pregnancies, recruited between March 1, 2014 and June 30, 2017 from the Mission Bay and San
102 Francisco General Hospital (SFGH) hospitals at UCSF that serve a racially and socioeconomically diverse
103 population. Our study population consists of 31.5% Non-Hispanic White women, 20.7% Hispanic/Latinx women
104 and 33.6% earns less than \$100,000/year. Additional demographic data and data from medical records are shown
105 in Tables S1 and S2.

106

107 Table 1: Demographics of the CIOB cohort (N = 295) from San Francisco, CA. When a variable is shown as
108 “missing”, it indicates that the participant did not answer that question in the questionnaire. The numbers in the
109 parentheses show the percentages (%) and standard deviations (std) as indicated in the table.

Baseline demographic, n (%)	Population 295 (100)
Maternal age, y (std)	33.2 (5.1)
Gravidity, n (std)	2.4 (1.6)
Ethnicity group 1 (%)	
African American or Black	3.7
American Indian or Alaskan Native	1.4
Asian or Asian American	11.2
White	31.5
Other	15.6
Missing	36.6
Ethnicity group 2 (%)	
Hispanic/Latino	20.7
Non-Hispanic	50.5
Missing	28.8
Income (%)	
< \$40,000	21.4
\$40,000-\$99,999	12.2
> \$100,000	65.1
Missing	1.3

110

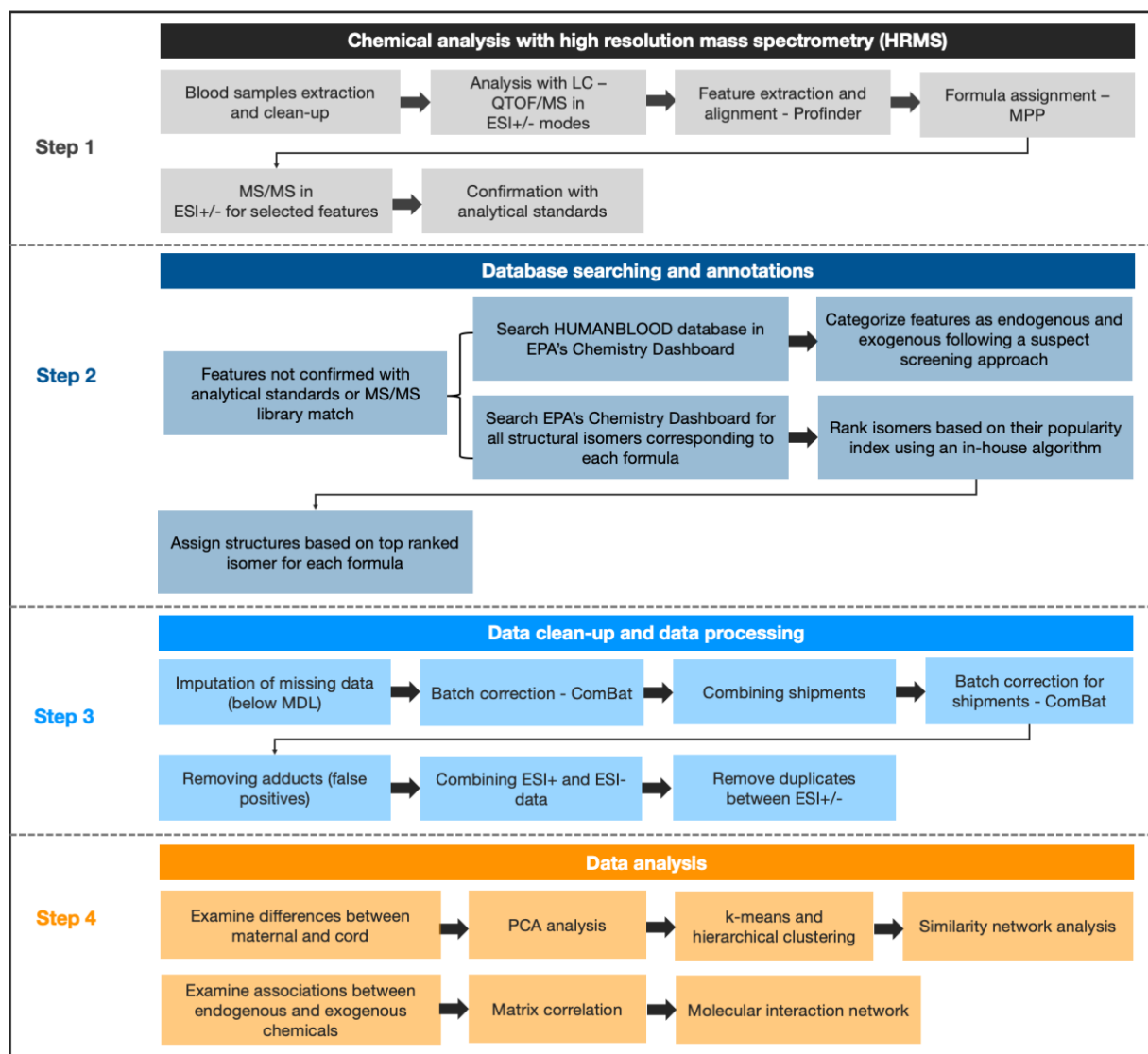
111

112 2.2 Non-targeted analysis workflow

113 Our non-targeted analysis workflow consisted of four main steps: i) chemical analysis, ii) database
114 searching and annotations, iii) data clean-up and processing, and iv) data analysis (Fig. 1). Briefly, we analyzed
115 serum samples with high resolution mass spectrometry and deduced chemical formulas from the detected
116 molecular masses. We conducted MS/MS fragmentation for selected chemicals and tentatively confirmed the
117 presence of a chemical by matching the experimental spectrum to database spectra, including experimental and *in*
118 *silico* predicted spectra. We then used analytical standards for a select number of chemicals to confirm with the
119 highest level of confidence. For our annotations, we employed the annotation scheme proposed by Schymanski et
120 al.¹⁹, where level 1 annotations are confirmed chemicals with analytical standards, level 2 annotations are
121 tentative identifications with MS/MS spectra, level 3 annotations have some diagnostic evidence based on
122 literature and data sources, and level 4 annotations are just molecular formulas without proposed structures. We
123 examined the presence of the chemicals in chemical databases to search for potential matches to industrial uses.
124 The details of the analytical method are described in the sections below.

125 In an attempt to navigate the complexity and high dimensionality of non-targeted analysis datasets, we
126 selected and applied various software tools that helped us analyze our data and interpret our findings. The
127 selection of the software packages was done based on the specific aims we tried to address in every step in our
128 workflow (Fig. 1). When selecting software packages, we had to consider the capabilities of the software to
129 address the aims of our study. For our purposes, we used i) commercial software (e.g., Agilent software packages)
130 when available and suitable, ii) open-source tools if their application made an important contribution or offered a
131 different approach compared to the commercial software (e.g., MS-Dial and different MS/MS databases), and iii)
132 in-house built algorithms if we were not able to find an existing tool that could help us tackle a certain challenge
133 in our study (e.g., level 3 annotations¹⁹ for man-made/industrial chemicals). In the sections below we provide an
134 explanation for the selection of each package.

135



137

138 Figure 1: Flowchart describing the individual steps of analyzing the maternal and cord samples and processing the
 139 collected data from our LC/QTOF nontargeted analysis.

140

141 2.3 Sample preparation

142 We analyzed 295 maternal and 295 matched cord blood samples (n total = 590). The blood samples were
 143 stored in the freezer at -80 °C at the University of California, San Francisco (UCSF). Prior to analysis, the samples
 144 were centrifuged (3000 rpm) to separate the serum from the red platelets. The serum samples were transported on

145 dry ice to the Environmental Chemistry Laboratory (ECL) of the Department of Toxic Substances Control
146 (DTSC) of California, in Berkeley, CA. The method is described in detail below and in our previous study.¹⁴
147 Briefly, aliquots of 250 μ L of serum were extracted by protein precipitation with methanol and the samples were
148 mixed and stored at 4 $^{\circ}$ C until they were analyzed with ultra-high pressure liquid chromatography – quadrupole
149 time-of-flight / mass spectrometry (UPLC-QTOF/MS). At the time of analysis, 10 μ L of extract were injected into
150 the UPLC-QTOF/MS system.

151 2.4 Instrumental analysis

152 The extracts were analyzed with an Agilent UPLC coupled to an Agilent 6550 QTOF (Agilent
153 Technologies, Santa Clara, CA) operated in both positive and negative electrospray ionization modes (ESI+ and
154 ESI-). Full scan accurate mass spectra (MS) were acquired in the range of 100-1000 Da with resolving power of
155 40,000 and a mass accuracy of <5 ppm. The MS/MS fragmentation ion spectra (MS/MS) were collected at 10, 20
156 and 40 eV collision energies and a mass accuracy of 10 ppm. The QTOF was calibrated before each batch and the
157 mass accuracy was regularly corrected with reference standards of reference masses 112.985587 and
158 1033.988109. The UPLC was operated with an Agilent Zorbax Extend-C18 column (2.1 x 50 mm, 1.8 μ m) and a
159 gradient solvent program of 0.3 mL/min with 5 mM ammonium acetate in 90% methanol/water increasing the
160 organic phase from 10% to 100% over 15 min, following a 4 min equilibration at 100%.

161 The collected data from the total ion chromatograms (TIC) were processed with Agilent MassHunter
162 Profinder for feature extraction. The features were then aligned using Mass Profiler Professional (MPP) across all
163 batches and the features found in blanks were subtracted from the samples. The features were matched to
164 formulas via screening with an in-house database of 2,420 unique formulas. The database was originally compiled
165 to contain 3,535 structures of exogenous chemicals of interest based on a literature search and expert curation.
166 Briefly, the database was compiled with the purpose of gathering manmade chemicals of high production volumes
167 and chemicals of concern for environmental health scientists due to their potential for adverse health effects. The
168 original database and the steps for its compilation are presented in our previous study.¹⁴ However, in this study,
169 we expanded our database by including all isomers corresponding to the 2,420 formulas and could be found on
170 EPA's Dashboard²⁰. After collecting all structural isomers, the updated version of the database contained 65,535

171 compounds (Supporting Spreadsheet 0-database). The updated version of the database contains both endogenous
172 and exogenous compounds, however, the vast majority of the features are exogenous. Matched features were
173 evaluated based on mass accuracy and isotopic pattern. Features of interests were prioritized for validation of
174 identification with data dependent acquisition and with targeted MS/MS. The MS/MS spectra of the prioritized
175 features were reviewed by empirical check of possible fragmentation peaks and were compared with spectra in
176 online experimental MS/MS databases: MassBank of Europe and North America²¹⁻²³, Human Metabolome
177 Database (HMDB)^{24,25} and mzCloud²⁶ and with support from *in silico* fragmentation tools: CFM-ID^{27,28}
178 (Competitive Fragmentation Modeling for Metabolite Identification).

179 The acquired spectra were then used to search both experimental and *in silico* databases for potential
180 matches with at least one fragment peak, aside from the molecular ion, and within a mass error of 10 ppm. We
181 limited our search to chemical features for which we could observe a clear chromatographic peak for the
182 molecular ion and for which the isotopic pattern match gave a score of 70 or higher. We then used the top
183 candidate structure proposed by the software to annotate the chemical features for which we found potential
184 matches.

185 In addition to MassHunter Profinder, we also utilized MS-Dial²⁹, which is an open source software for
186 high-resolution mass spectrometry (HRMS) data processing and it was developed at University of California,
187 Davis and the RIKEN Center for Sustainable Resource Science (Japan).²⁹ Adding MD-Dial to our search, enabled
188 us to expand our search with additional databases. For MS-Dial, we used the same software parameters as for
189 MassHunter Profiler (Supporting Spreadsheet 1). The databases we used were: “All public MS/MS databases for
190 positive MS/MS” (13,303 unique compounds) and “All public MS/MS databases for negative MS/MS” (12,879
191 unique compounds).

192 Finally, matched chemical features were further compared with purchased reference standards for
193 confirmation. The confirmation with chemical standards was done by comparing the retention times (RTs) and the
194 MS/MS spectra of the chemical feature in the sample to the analytical standard. The selection of features for
195 confirmation with analytical standards is described in detail in our earlier study.¹⁴

196 [2.5 Quality assurance \(QA\) / Quality control \(QC\)](#)

197 Extraction blanks, spike blanks and QC samples were included with each set of 20 extracted samples.
198 Every batch analyzed with LC-QTOF/MS was accompanied by a water blank, a matrix blank and a matrix spike
199 analyzed in the same sequence. QC samples were used to monitor the instrument's performance by inspecting RT
200 shifts, changes in mass accuracy and changes in peak intensity. In ESI+, we used triphenyl phosphate D15 and
201 DL-cotinine (methyl D3) as internal standards, while in ESI-, we used Perfluoro-n-[1,2-13C2] octanoic acid
202 (M2PFOA). We used blank samples to correct the abundances of the chemical features and to remove features for
203 which the abundances in the samples were not higher than two times that found in the blanks. The blanks
204 consisted of LCMS grade ultraclean water (Water, Burdick & Jackson™ for HPLC, LC365-1) and were
205 processed in the same way as the samples. The QC samples consisted of commercially available human AB
206 serum (Corning™ Human AB Serum, 35060CI) spiked with 7 poly and perfluoroalkyl substances (PFAS) and 6
207 organophosphate flame retardants (OPFRs) (Supporting Spreadsheet 1: QC samples) at 10 ng/ml. The QC
208 samples were treated in the same way as the real samples and followed the same process (Supporting Spreadsheet
209 1).

210 2.6 Database searching for feature annotation

211 We used a suspect screening approach for annotation. First, we searched the HUMANBLOOD database
212 in EPA's Chemistry Dashboard²⁰, which contains chemicals that are endogenous and have been previously
213 detected in human blood. The database is an aggregate from public resources, including the Human Metabolome
214 Database (HMDB)²⁴, WikiPathways³⁰, Wikipedia³¹ and literature articles²⁰. The database excludes metals, metal
215 ions, gases, drugs and drug metabolites. Screening this database allowed us to distinguish between features that
216 are more likely to be endogenous and features that are more likely to be exogenous. To do that, we searched every
217 formula in the database and marked the ones that had a hit in the database. Then, we labeled all features
218 corresponding to these formulas as endogenous and the remaining as exogenous. The rationale behind this
219 approach is that since we know we are analyzing blood samples and HUMANBLOOD is an extensive database
220 about all endogenous compounds that have been previously detected in blood, if a detected feature in our samples
221 has a formula that is present in the HUMANBLOOD database, then that feature is most likely an endogenous
222 compound. We then searched the HUMANBLOOD database for all isomers corresponding to our endogenous

223 formulas and the remaining databases in EPA's Chemistry Dashboard for all isomers corresponding to our
224 exogenous formulas. We then applied an algorithm developed by the first author, Dr. Abrahamsson, to rank the
225 isomers of each formula based on (i) total number of available isomers on the Dashboard, (ii) the number of data
226 sources in the Chemistry Dashboard, (iii) number of PubChem data sources, and (iv) number of PubMed
227 publications. We then used the top ranked isomer to annotate the chemical features that were not confirmed with
228 MS/MS spectra matching or with analytical standards. For example, searching $C_8HF_{17}O_3S$ gives us two isomers:
229 perfluorodecanoic acid and perfluoro-3,7-dimethyloctanoic acid. If we were to randomly select one of the isomers
230 our probability of picking the right isomer would be 0.5. Then, making the assumption that more prevalent
231 isomers have a higher number of literature and data sources, we can adjust that probability by taking into account
232 that information after normalizing all numbers for (ii), (iii), and (iv) from 0-1. So, while the probability of
233 randomly picking the right isomer for $C_8HF_{17}O_3S$ is 0.5, perfluorodecanoic acid has a higher probability (0.73) of
234 being the right isomer because it has more literature and data sources than perfluoro-3,7-dimethyloctanoic acid
235 (0.27). It is important to acknowledge that these estimates are amenable to change as EPA's Chemistry Dashboard
236 is a dynamic project and keeps being updated with additional chemicals. Furthermore, these annotations may be
237 susceptible to the Matthew effect³², where researchers prioritize chemicals to study mainly because other
238 researchers have prioritized the same chemicals. However, since these are just annotations and serve only in
239 providing diagnostic evidence for the identification of chemical compounds, we deemed them as sufficient for
240 that purpose. The code for the algorithm is available on GitHub
241 (<https://github.com/dimitriabrahamsson/nontarget-maternalcord.git>).

242 In order to evaluate the effectiveness of the algorithm, we compared the level 3 annotations of the
243 algorithm to the level 1 and 2 annotations and observed how many times the predictions of the algorithm agreed
244 with the level 1 and 2 annotations (Supporting Spreadsheet 1: algorithm validation). Although the level 3
245 annotations are just annotations and not confirmations, in some cases they can be very informative and help
246 compose a diagnostic picture for the underlying structure of a detected chemical feature. This is particularly
247 helpful for certain chemicals that are more targetable than others. For instance, the presence of fluorine in a
248 formula would indicate that this compound is an exogenous compound and it most likely belongs to the category

249 of poly and perfluoroalkyl substances (PFAS). Another example is when a chemical formula has only a limited
250 number of potential isomers (e.g., 5-10 isomers) and all potential isomers are endogenous compounds with very
251 similar function and properties (e.g. chenodeoxycholic acid).²⁰

252 2.7 Data clean-up and data processing

253 2.7.1 Imputation of values below detection limit

254 To impute below detection limit values, we used a computational approach which assigned missing
255 values based on the distribution of the data points. We log transformed the data from the MS analysis for each
256 chemical across samples and calculated the median, the minimum and the standard deviation of the distribution.
257 We then fit a normal distribution to the data points based on the median and the standard deviation that we
258 calculated from the experimental data. The model then generated random values between the minimum measured
259 experimental value (~5,000) and the absolute minimum (0). The minimum measured value is dependent on the
260 cut-off point set in the software during the first processing steps of the chromatograms. Since in non-targeted
261 analysis studies the true method detection limit is unknown, this cut-off point is set so that it represents a safe
262 margin from the baseline of the chromatogram. So, for example, if the abundance for the baseline is 1,000 then
263 the cut-off point is set as 5 x 1,000. The code for the imputation is available as supporting information on GitHub
264 (<https://github.com/dimitriabrahamsson/nontarget-maternalcord.git>)

265 2.7.2 Batch correction

266 We analyzed 590 samples in total consisting of 295 maternal and 295 cord blood samples. The samples
267 were analyzed in two shipments of approximately 300 samples (150 maternal samples and 150 cord samples) in
268 each shipment. Within a shipment, the 300 samples were analyzed in 15 batches yielding 20 samples per batch
269 (15 batches x 20 = 300). Each batch of 20 consisted of 10 maternal and 10 cord blood samples. Before the
270 analysis, the samples were randomized, however, in every batch, the maternal samples were analyzed with their
271 corresponding cord samples in order to avoid introducing additional batch effects between maternal and cord
272 samples. To clarify even further, the maternal and cord samples within each batch were randomized and were not
273 analyzed in pairs of maternal and cord. To correct the abundances of the chemicals measured in the samples for

274 batch effect, we employed the ComBat package for python³³. ComBat uses a parametric and non-parametric
275 Bayes framework to adjust the values for batch effects. The method requires that the batch parameter is known
276 and that the data are log transformed (method is described in detail in Johnson et al.³⁴). For our dataset, we first
277 applied the ComBat package to each shipment separately to correct for batch effect within shipment. Then we
278 applied the package again to correct for batch effect across shipments.

279 2.7.3 Combining shipments

280 As our samples were analyzed in two separate shipments of approximately 150 samples each, one of the
281 challenges was to combine the two datasets of the two shipments, given the potential shifts in RT and differences
282 in peak alignment. This step was done after batch correction for within shipment variability. In order to address
283 this issue, we grouped all chemical features by their formulas and sorted them by ascending RTs. We then created
284 an index for each group of formulas (1, 2, 3, etc.), which we then used to create an identifier based on the formula
285 and the position of each isomer in the index. For example, if the formula C₅H₁₃NO had three isomers, the first
286 isomer was named C5H13NO_1, the second isomer as C5H13NO_2 and the third isomer as C5H13NO_3. We
287 then merged the two datasets on the identifier and removed features that were present in only one of the datasets.
288 We examined the difference in the RT and molecular mass and removed those features for which RT differed by
289 more than 0.5 min or where the mass difference was more than 15 ppm. A limitation associated with this
290 approach is that there could be cases where we are removing valid features if the molecular formula assigned in
291 one shipment does not match the molecular formula assigned in the other shipment. This would then lead to false
292 negatives and can result in underestimating the number of truly detected compounds. This would be more likely
293 to happen in instances where multiple formulas can be assigned to a given chemical feature. This challenge
294 warrants further exploration to ensure that we can leverage the full potential of NTA datasets.

295 2.7.4 Removing adducts

296 Electrospray ionization adducts are chemicals that are formed inside the instrument during analysis of the
297 samples as the salts ions from the electrolytes used to enhance ionization bind to the ions of the organic molecules
298 formed during electrospray ionization. We filtered out these chemicals by identifying the features that strongly

299 correlate ($r > 0.5$) with each other and have distinct mass differences corresponding to salt ions, such as sodium
300 (Na^+), potassium (K^+), formate (HCOO^-) and ammonium (NH_4^+). Na^+ and K^+ adducts particularly important in
301 serum analysis as these elements occur naturally in the human body and can form adducts with analytes during
302 ionization. For filtering out adducts, we used a mass accuracy filter of 15 ppm.

303 2.8 Data Analysis

304 2.8.1 Abundance and frequency calculations

305 We examined the relationship between chemical features in maternal samples and cord samples in terms
306 of abundances and detection frequencies. For the abundances, we used the mean log transformed abundance of
307 each chemical in maternal samples and compared it to the corresponding feature in the cord samples using a linear
308 regression model. For the detection frequencies, we used a universal abundance cutoff of 5,000, which is
309 comparable to the minimum measured value in the chemical features (~ 5000). We compared the detection
310 frequencies of the chemical features between maternal and cord samples both in terms of kernel density estimates
311 and in terms of absolute numbers. We also examined the differences in detection frequencies of endogenous and
312 exogenous chemical features.

313 2.8.2 Unsupervised clustering

314 We conducted a principal component analysis (PCA) to examine the differences in the PCs between
315 maternal and cord samples. We then conducted a correlation analysis, where we examined the relationship of the
316 first 3 PC components with technical features and clinical covariates, i.e., batch, shipment, sample type
317 (maternal/cord) and gestational age group (preterm/full-term). We identified the features that were differentially
318 enriched in maternal and in cord blood samples by comparing the abundances of the chemical features in maternal
319 samples to those of cord samples and marking the features that showed a significant trend to be higher in maternal
320 and lower in cord and vice versa ($p < 0.05$) after correcting for multiple hypothesis testing using the approach of
321 Benjamini-Hochberg with a false discovery rate of 5%. We checked the cluster stability by comparing the PC1
322 values of the maternal samples to the PC1 values of the cord samples using a two-sided Mann-Whitney-Wilcoxon
323 test with Bonferroni correction.

324 2.8.3 Network analysis for maternal and cord samples

325 The purpose of the network analysis was to assess whether maternal samples are more similar in terms of
326 chemical abundances to their corresponding cord samples than to other maternal samples. For this analysis, we
327 considered two network-based approaches.

328 For the first approach, we conducted a matrix correlation of all samples using a linear regression model
329 and calculated the correlation coefficients and p-values. We then adjusted the p-values by applying a multiple
330 hypothesis correction using the Benjamini-Hochberg correction with a false discovery rate of 5% and we marked
331 the maternal and cord sample pairs that remained significant after the multiple hypothesis correction. We then
332 plotted the correlations as a correlation network using the NetworkX³⁵ package for Python. We then divided the
333 network into four subnetworks i) correlations between matched maternal-cord pairs only, ii) correlations between
334 unmatched maternal cord pairs and between maternal only and cord only, iii) correlations between maternal
335 samples only, and iv) correlations between cord samples only. We then calculated the number of connections in
336 each subnetwork and the averages correlation coefficient for each subnetwork and compared the subnetworks to
337 each other.

338 For the second approach, we carried out permutation analysis randomly picking a matched pair of a
339 maternal and cord samples (M1 and C1), and a random maternal sample (M2) 100 times. For each iteration, we
340 then calculated the abundance ratios of all chemical features for every sample pair (M1-C1, M1-M2 and M2-C1).
341 Chemical features with ratios in the range of 0.75 – 1.25 were considered “similar” chemical features between
342 two samples. We calculated the number of chemicals for each pair and compared them to each other. We
343 calculated the average number of similar chemicals for every pair and compared the pairs to each other. The code
344 is available on GitHub (<https://github.com/dimitriabrahamsson/nontarget-maternalcord.git>).

345 2.8.4 Partitioning of chemical features between maternal and cord

346 As part of our analysis, we wanted to understand why different chemicals exhibit different partitioning
347 behaviors between maternal and cord blood. We examined the partitioning behavior of the detected chemical
348 features between maternal and cord by calculating the cord/maternal abundance ratio (R_{CM}) as:

349

$$R_{CM} = \frac{A_c}{A_m}$$

350

where, A_c is the abundance of a chemical feature in cord blood and A_m is the abundance of a chemical in

351

maternal blood. R_{CM} has been previously described in environmental chemistry studies³⁶⁻³⁸ as:

352

$$R_{CM} = \frac{C_C}{C_M}$$

353

where, C_C is the concentration of a given chemical in cord blood and C_M is the concentration in maternal blood.

354

Since concentrations are not available for all chemical features, we replaced concentration with abundance as

355

follows:

356

$$R_{CM} = \frac{C_C}{C_M} = \frac{\frac{A_c}{RRF}}{\frac{A_m}{RRF}} = \frac{A_c}{A_m}$$

357

where, RRF is the relative response factor used to calculate concentrations assuming a linear calibration curve.

358

It is important to note that R_{CM} does not describe an equilibrium partition ratio, such as the octanol-water

359

equilibrium partition ratio (K_{OW}), but rather a concentration ratio representing the current state of a dynamic

360

system. Considering that the placenta is a dynamic system, where chemicals are transported through passive

361

diffusion and active transport to and from the system, it is unlikely that any chemicals will be at thermodynamic

362

equilibrium. The partitioning of chemicals between cord and maternal blood has also been described as a

363

concentration ratio in previous studies.³⁶⁻³⁸

364

Previous studies have shown that the partitioning behavior of chemicals between maternal and cord blood

365

is related to the chemicals' physicochemical properties^{39,40} and to certain physiological parameters that can affect

366

the placenta, such placental aging⁴¹ and gestational diabetes⁴². In an attempt to understand the parameters

367

determining R_{CM} we used a linear regression model to assess its relationship to physicochemical properties and

368

physiological parameters. The physicochemical properties we used are known as the Abraham descriptors⁴³⁻⁴⁵ and

369

commonly used in quantitative structure-activity relationships (QSARs). These descriptors were: i) E, which

370

describes a chemical's ability to engage in London dispersion forces and dipole-induced dipole interaction; ii) S,

371

which describes a chemical's ability to engage in dipole-induced dipole and dipole-dipole interactions, iii) A,

372 which describes hydrogen bond acidity; iv) B, which describes hydrogen bond basicity; v) V, which is the
373 McGowan molecular volume; and vi) L, which is the hexadecane/air partition ratio. The Abraham descriptors
374 were obtained from the UFZ-LSER database of the Helmholtz Centre for Environmental Research-UFZ⁴⁶
375 (Zentrum für Umweltforschung). In addition to the Abraham descriptors, we also collected the K_{OW} of the
376 chemicals in the dataset and examined its relationship to R_{CM} . These calculations were only applied to chemical
377 features whose structures that were annotated with level 1-3 annotations.

378 The physiological parameters we used were the body-mass index (BMI), maternal age at delivery,
379 gestational age, birth weight and gestational diabetes (Table S2). Since R_{CM} is a chemical-specific parameter and
380 not a participant-specific parameter, in order to access its relationship to physiological parameters we calculated
381 R_{CM} for every chemical and every maternal-cord pair and then we calculated the average value per participant, as
382 a hypothetical R_{CM} representing the average R_{CM} of all chemicals in each participant.

383 2.8.5 Associations between endogenous and exogenous compounds

384 After calculating the number of exogenous and endogenous chemicals, as described previously in the
385 section for database searching, we examined the associations between endogenous and exogenous compounds
386 using the approach of molecular interaction networks. It is important to note that although these types of networks
387 are commonly known as “molecular interaction networks”⁴⁷⁻⁵⁰, the term “interaction” can be interpreted as in that
388 the chemical compounds are having an effect on one another or in the epidemiological sense that two parameters
389 are having an effect on one outcome. However, in this context, “interaction” refers to the associations between
390 chemical features. In NTA applications, the precise relationships are still speculative and the “interactions” shown
391 by these networks are proposed associations that need to be further explored and validated with experimentation.
392 One important advantage of these networks is that they allow for visualization of multiple endogenous and
393 exogenous features at once together with their inter- and intra- associations.

394 As a first step for our exercise, we applied a matrix correlation and calculated the correlation coefficients
395 and p-values between all endogenous and all exogenous chemical features after adjusting the p-values for multiple
396 hypothesis testing using the Benjamini-Hochberg approach and a false discovery rate of 5%. We applied the
397 approach of molecular interaction networks to visualize the associations and examine the relationships between

398 endogenous and exogenous compounds for the significant correlations between endogenous and exogenous
399 chemical features separately for maternal and cord samples. To build the network, we used Cytoscape⁵¹ with
400 Metscape⁵² as a plug-in. Cytoscape⁵¹ is an established tool in the field of bioinformatics and -omics research for
401 the visualization of networks and assisting in the discovery of underlying biological mechanisms. Due to the large
402 number of relationships and the complexity of the network, we focused our comparison on the chemical features
403 that had an annotation score > 0.3, or confirmed with MS/MS or analytical standards, and had a Pearson $|r| > 0.4$.

404 2.9 Statistical analyses

405 For all the correlations mentioned in the sections above we used Pearson r and we adjusted the calculated
406 p-values for multiple hypothesis testing using the Benjamini-Hochberg approach with a false discovery rate of
407 5%. When comparing two groups for statistically significant differences, such as in unsupervised clustering, we
408 used a two-sided Mann-Whitney-Wilcoxon test with Bonferroni correction.

409 3. Results

410 3.1 Chemical analysis with LC-QTOF/MS

411 The recursive feature extraction and formula matching for the 295 pairs of maternal and cord blood
412 samples (n total = 590 samples) resulted in 824 features in ESI- and 731 features in ESI+ for shipment 1, and 707
413 features in ESI- and 576 features in ESI+ for shipment 2. After combining the datasets for the two shipments, the
414 resulting dataset for ESI- summed up to 412 features and the dataset for ESI+ to 298 features (n total = 710
415 features) after filtering out the features that showed an RT difference of > 0.5 min or a mass difference of > 15
416 ppm. Combining the data from ESI- and ESI+, resulted in 712 features. This number is higher by 2 features
417 compared to the total number of ESI- and ESI+ because 1 isomer from ESI- had more than 1 possible matches
418 from ESI+ based on the criteria that we set for merging the two datasets (RT difference of 0.5 min and mass
419 accuracy of 15 ppm). Ten features were identified as duplicates between ESI- and ESI+ and were removed from
420 the dataset. Seventeen features were identified as adducts and were also removed from the dataset. The complete
421 datasets before (n = 712) and after clean-up (n = 685) are presented in Supporting Spreadsheet 1 (sheets: dataset
422 1.0 and dataset 2.0). We confirmed 19 unique compounds with analytical standards, we tentatively identified 73

423 compounds with MS/MS spectra and annotated 98 compounds using our annotation algorithm (Supporting
424 Spreadsheets 1: level 1-2 and level 3-4).

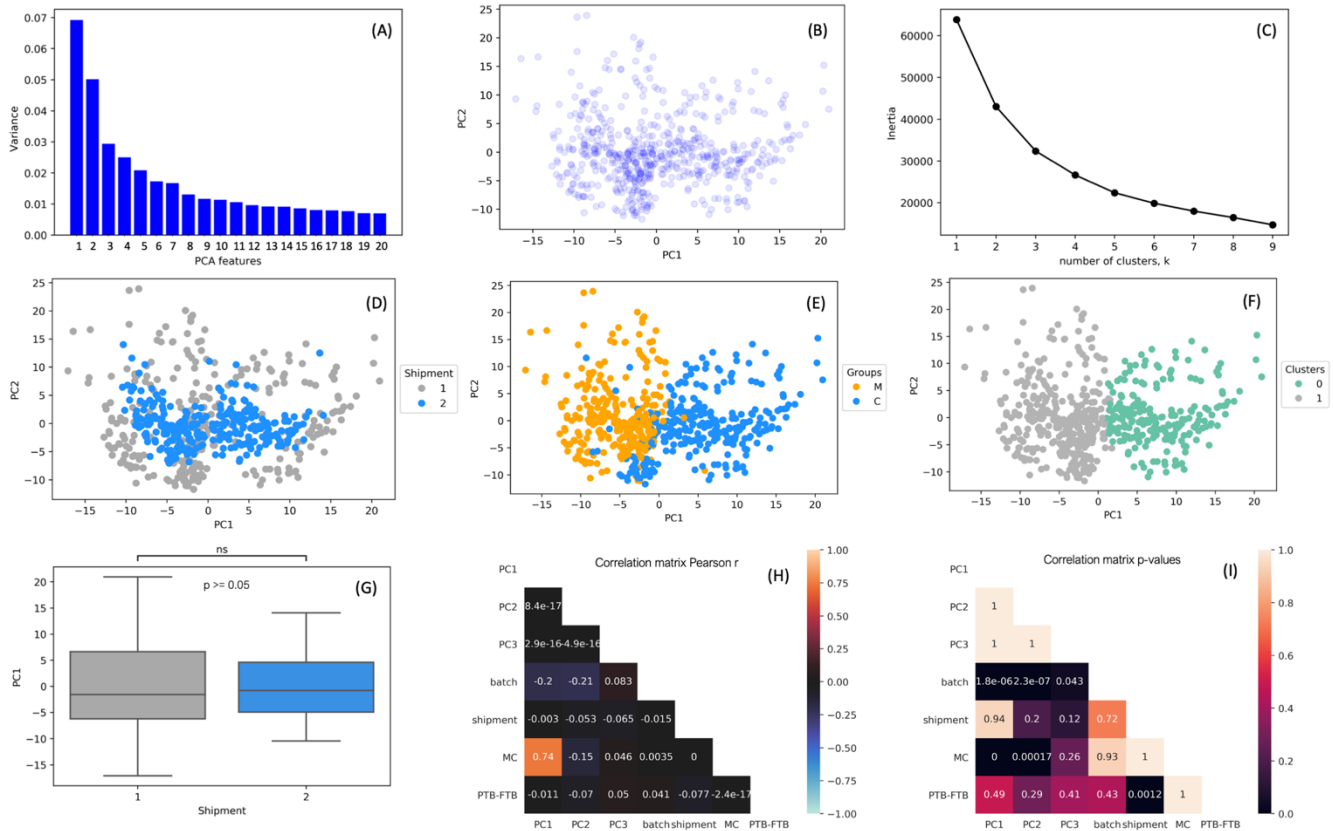
425 3.2 Database searching for feature annotation

426 We annotated 142 features as endogenous compounds and the remaining 543 features as exogenous
427 compounds. Among the chemical compounds with the highest annotation scores, we found 5 PFAS:
428 perfluorohexanesulfonic acid (PFHxS), perfluorooctanesulfonic acid (PFOS), perfluorodecanoic acid (PFDA),
429 perfluoroundecanoic acid (PFUnDA) and perfluorononanoic acid (PFNA); and 2 cyclic volatile methylsiloxanes:
430 octamethylcyclotetrasiloxane (D4) and decamethylcyclopentasiloxane (D5) (annotations with the individual
431 scores in Supporting Spreadsheet 1: level 3-4). PFDA, PFNA, PFHxS and PFOS were also confirmed with
432 analytical standards (Supporting Spreadsheet 1: level 1-2). When we evaluated the performance of the algorithm
433 used for the level 3 annotations, we observed that for compounds with annotation scores from 1-0.3, the algorithm
434 predicted correctly 16 out of the 22 formulas that were common between level 3 and level 1 and 2 annotations,
435 corresponding to an accuracy of 73% (Supporting Spreadsheet 1: algorithm validation). For compounds with an
436 annotation score of 0.3-0.1, the accuracy of the algorithm was 50% and for compounds with annotation score <0.1
437 the accuracy dropped to 8%. As anticipated, higher annotation scores were more likely to give a correct
438 prediction. We, therefore, considered as level 3 annotations only the compounds that had an annotation score >
439 0.3.

440 3.3 MS data clean-up and data processing

441 In the original dataset before batch correction, we observed two distinct clusters that corresponded to the
442 two shipments (Fig. S2 A-F). Following a matrix correlation, we observed strong correlations between the first 3
443 PCs and the parameters corresponding to batch number, shipment, and sample type (maternal vs cord) (Fig. S2 I).
444 In addition, we observed significant differences in the PCs between shipment 1 and shipment 2 (Fig. S2G), and
445 significant differences in the PCs between maternal and cord samples (Fig. S2H). Batch correction with ComBat
446 removed the largest part of the effects related to batch and shipment (Fig. 2D), while maintaining the differences
447 between maternal and cord (Fig. 2E). The updated plots after batch correction (Fig. 2) also showed that there were

448 two main clusters of samples (Fig. 2C and 2F) that corresponded to the maternal and cord sample groups (Fig.
 449 2E).
 450
 451



452
 453 Figure 2: Results of the data analysis after batch correction with ComBat for the two shipments and the batches
 454 within each shipment. The samples were first corrected for the batches within shipment and then for the two
 455 shipments. (A): PCA features and the variance explained (%); (B) PC1 and PC2 as a scatterplot; (C)
 456 approximation of the optimal number of clusters in the dataset; (D) PC1 and PC2 color-coded by shipment; (E)
 457 PC1 and PC2 color-coded by sample type – maternal vs cord blood; (F) agnostically derived clusters using a k-
 458 means algorithm; (G) boxplot for PC1 by shipment (the error bars show the 10th and 90th percentiles, the boxes
 459 show the 25th and 75th percentiles and the middle line shows the median); (H) Pearson r values and p-values (I) for
 460 matrix correlation for PC1-3, batch, shipment, sample type maternal vs cord and full term vs preterm birth.
 461

462

463

464

465 3.4 MS data analysis

466 3.4.1 Differences between maternal and cord

467 The maternal and cord samples showed similar profiles of detection frequency with the largest cluster of
468 chemical features appearing at 80-100% frequency (Fig. 3B-C). We observed an overall good agreement ($r =$
469 0.93) between the mean log abundances of the chemical features in the maternal samples and the chemical
470 features in the cord samples with some chemical features deviating from the regression line (Fig. 3A). In addition,
471 in both maternal and cord samples the number of exogenous compounds was about 3 times higher than that of
472 endogenous (Fig. 3D-E). This is expected considering that the vast majority of the chemicals in our database are
473 exogenous.

474 We observed significant differences in PC1 between maternal and cord samples both before (Fig. S2E and
475 S2H) and after batch correction (Fig. 2E and 2H). Removing the batch effect accentuated the differences between
476 maternal and cord samples (Fig. 2E and 2H).

477

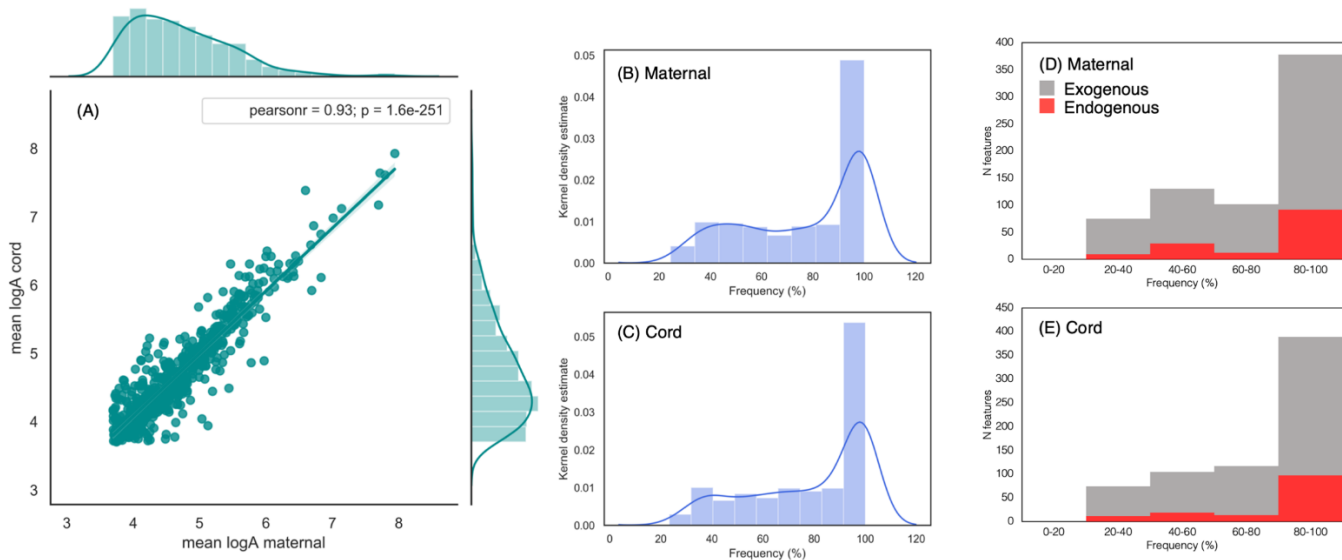
478

479

480

481

482



483

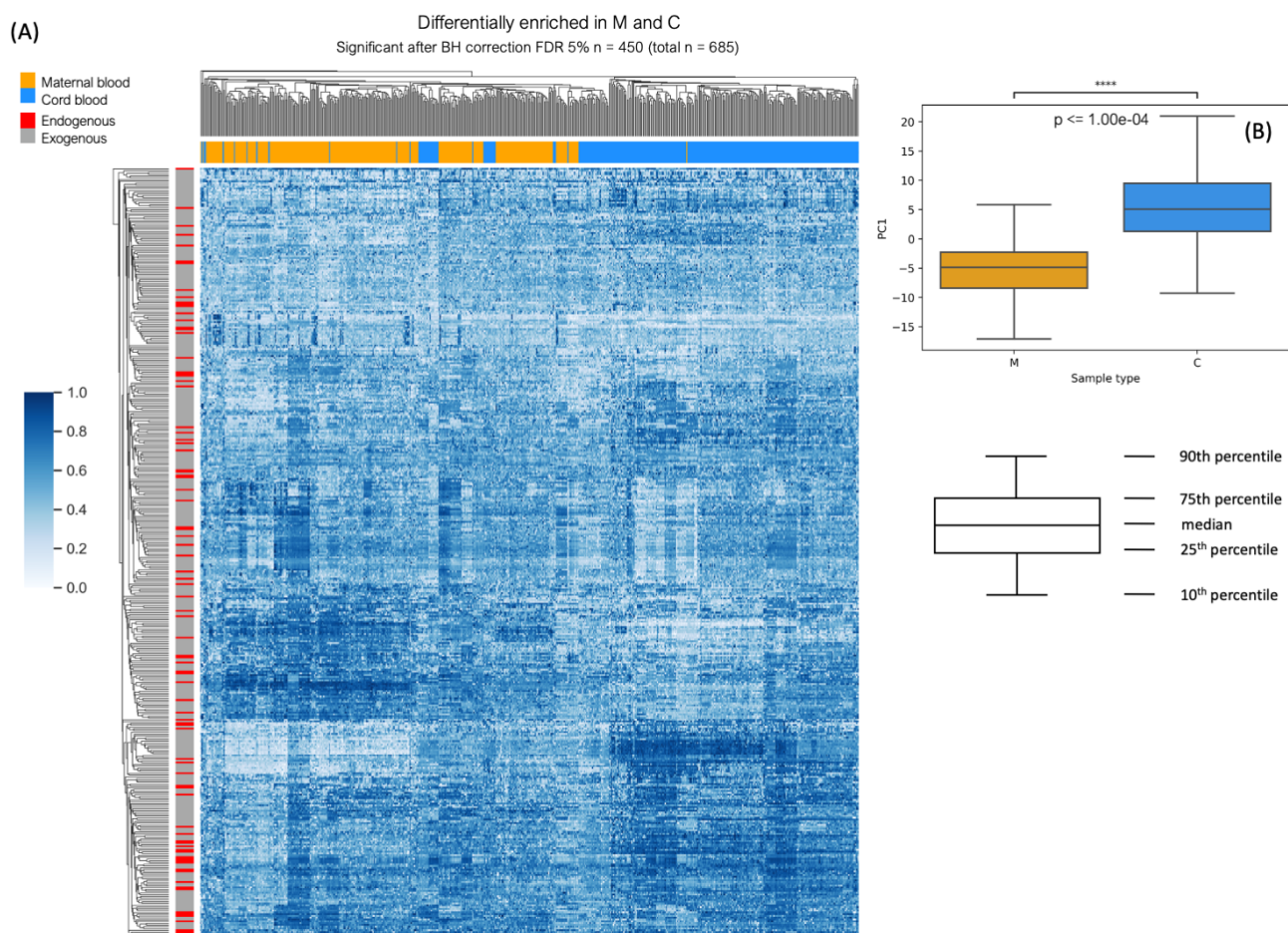
484 Figure 3: Correlation between maternal and cord abundances (A) (in log scale) and detection frequency
 485 calculations with kernel density curves for chemicals in maternal (B) and cord (C) blood samples (N=295
 486 chord/maternal). The figure also displays the detection frequency for maternal (D) and cord (E) color-coded as
 487 endogenous and exogenous compounds.

488

489

490 Out of 685 chemical features detected in MS analysis after filtering (as described in the methods above),
 491 450 showed a significant difference between maternal and cord samples (Fig. 4). We observed clear clustering
 492 between maternal and cord blood samples indicating a sufficient difference in the chemical composition between
 493 maternal and cord samples for them to be classified as two distinct clusters (p-value for PC1 between maternal
 494 and cord ≤ 0.0001 ; Fig. 4B).

495



496

497 Figure 4: Clustering heatmap for maternal and cord blood samples and the chemical features that showed a
 498 significant trend to be higher in maternal or cord after multiple hypothesis correction (Benjamini-Hochberg test,
 499 5% false discovery rate). Out of 685 chemical features in total, 450 showed a significant difference. The samples
 500 are color-coded by sample type (maternal vs cord). The features are color-coded by chemical type (endogenous vs
 501 exogenous). The error bars in the box-plot show the 10th and 90th percentiles, the boxes show the 25th and 75th
 502 percentiles and the middle line shows the median.

503

504 Our similarity network analysis using a correlation network showed that paired maternal and cord
 505 samples had a higher number of significant correlations (N = 170; Fig. S3 A) compared to unpaired maternal and
 506 cord samples (N = 84; Fig. S3 B) and compared to maternal only (N=41; Fig. S3 C) and cord only (N=41; Fig. S3

507 D). No significant differences were observed in the average $|r|$ values between the four groups. Our similarity
508 network analysis using a permutation approach showed a very similar trend (Fig. S4). The average of 100
509 iterations showed that paired maternal and cord samples (M1-C1) shared more similar chemical features
510 compared to maternal – maternal pairs (M1-M2) and unmatched maternal – cord samples (M2-C1) (Fig. S4).

511 We observed that the majority of R_{CM} values are concentrated around 1 indicating an even partitioning
512 between maternal and cord blood (Fig. S5 A and S5 B). R_{CM} showed a weak but significant positive correlation
513 with RT (S5 D). No significant correlation was found for R_{CM} and molecular mass (S5 C). We also observed a
514 significant positive association between R_{CM} and E (Fig. S6 A), a significant negative association between R_{CM}
515 and K_{OW} (Fig S6 G), and a significant positive association between K_{OW} and RT (Fig. S6 H). We observed a
516 borderline significant association between R_{CM} and gestational age (p-value = 0.07) (Fig. S7) and the median of
517 the overall R_{CM} values were slightly higher in preterm birth samples compared to full term and late term. A
518 slightly elevated median value was also observed for the gestational diabetes samples, although there was no
519 statistically significant difference between cases and controls (Fig. S7).

520 3.4.2 Correlations between endogenous and exogenous compounds

521 We observed 21,522 significant relationships between features that were annotated as endogenous and
522 features that were annotated as exogenous in maternal samples and 19,846 in cord samples after multiple
523 hypothesis correction (n total relationships = 77,106 in maternal and n = 77,106 in cord samples, Fig. S8). From
524 the significant relationships, 103 relationships in maternal and 128 relationships in cord samples had an absolute
525 Pearson $r > 0.5$, 5 relationships in maternal and 4 relationships in cord samples had an absolute Pearson $r > 0.7$
526 and 1 relationship in maternal and 1 relationship in cord samples had an absolute Pearson $r > 0.8$ (dataset with the
527 calculated r and p-values in the Supporting Spreadsheet 2).

528

529

530

531

532

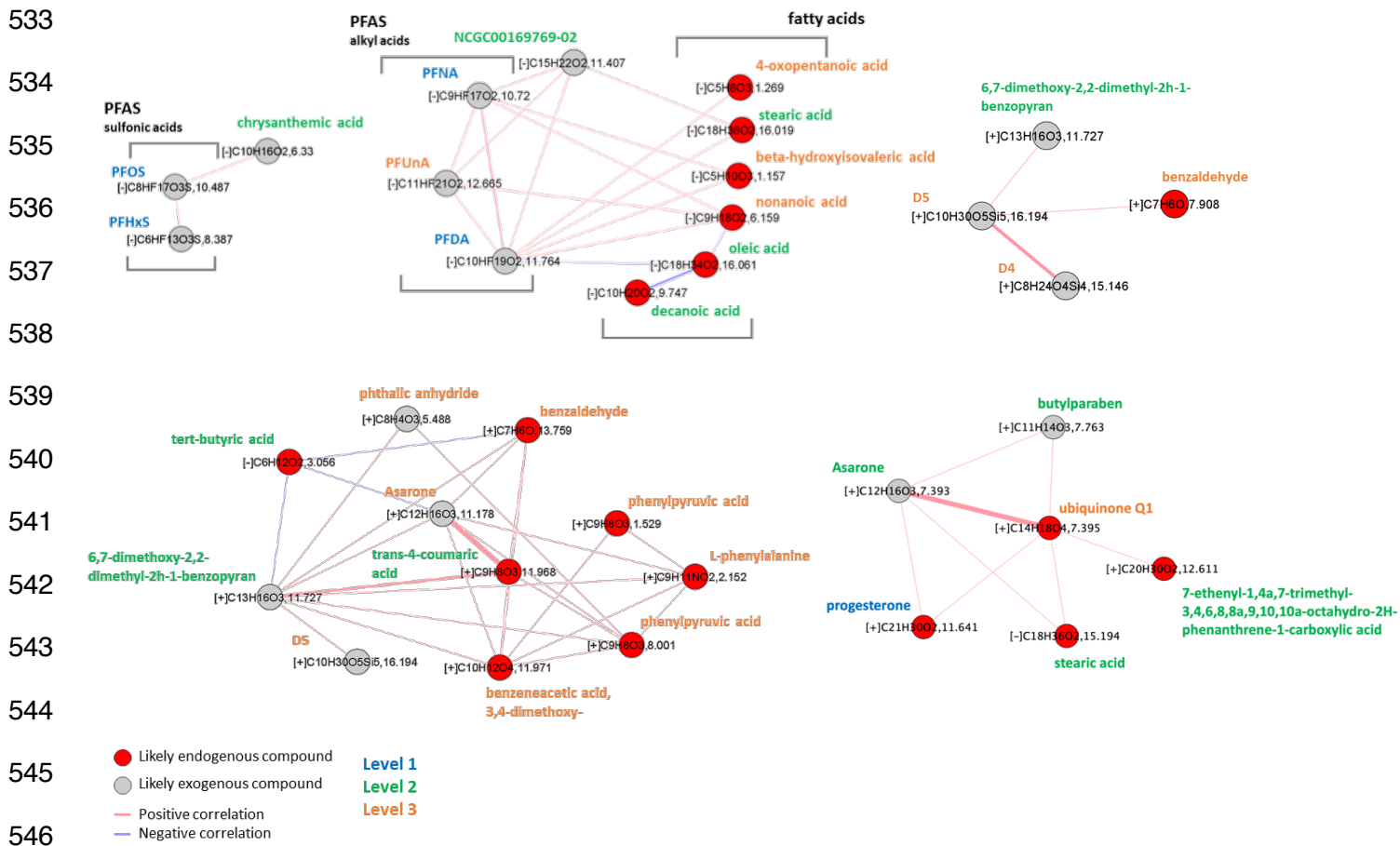
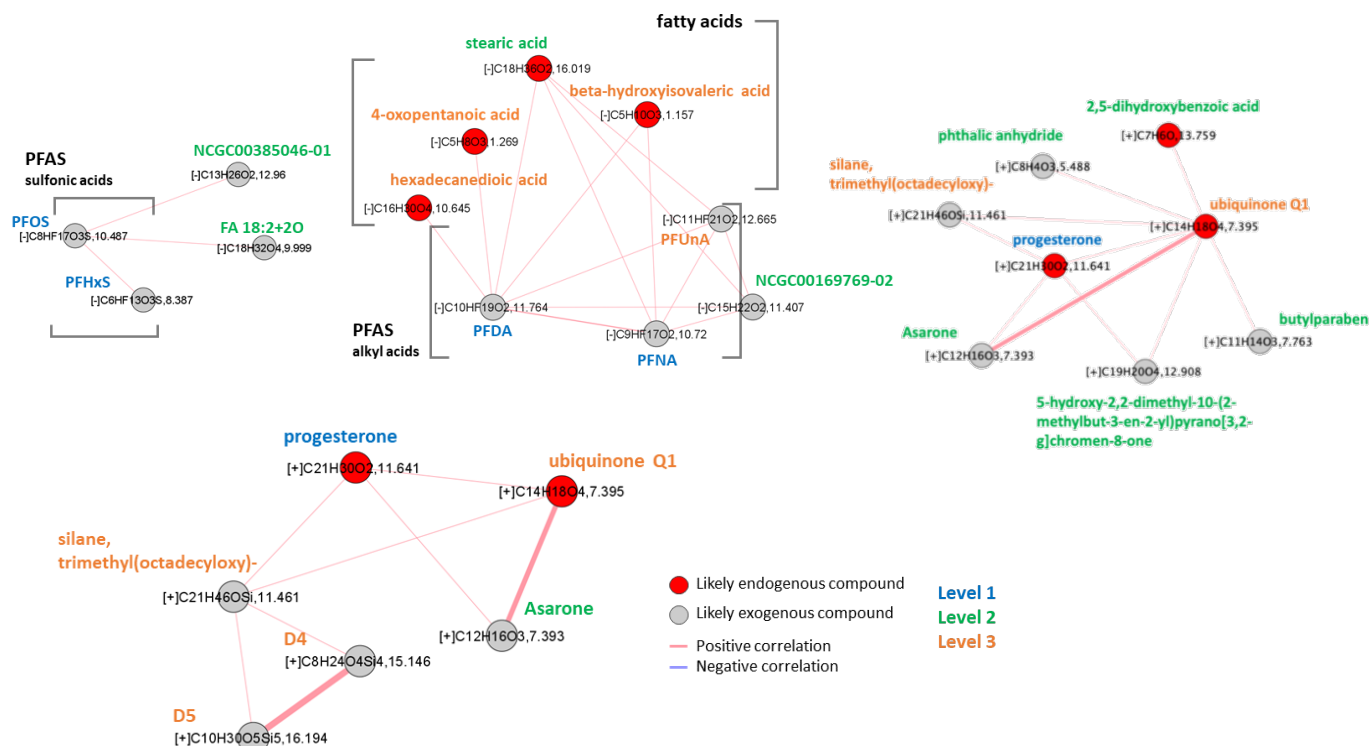


Figure 5: Molecular interaction networks for endogenous (red) and exogenous (gray) chemical features in the maternal blood samples (N = 295). The network shows the features which had an annotation score of > 0.3 or were identified with MS/MS or with analytical standards. The network shows the correlations with an absolute $r > 0.4$. The red lines indicate positive correlations and the blue lines indicate negative correlations. The thickness of each line indicates the strength of the correlation ($|r| = 0.4 - 1$). The different colors in the names of the chemicals correspond to the annotation levels of Schymanski et al.¹⁹ showing confidence in annotation. Level 1 are compounds that have been confirmed with analytical standards, level 2 are compounds that have been tentatively identified with MS/MS spectra matching and level 3 are compounds for which we have a definitive formula and some diagnostic evidence based on our annotation algorithm described in materials and methods.

559
560
561
562
563
564
565
566
567
568
569
570
571



572 Figure 6: Molecular interaction networks for endogenous (red) and exogenous (gray) chemical features in the cord
573 blood samples (N = 295). The network shows the features which had an annotation score of > 0.3 or were
574 identified with MS/MS or with analytical standards. The network shows the correlations with an absolute $r > 0.4$.
575 The red lines indicate positive correlations and the blue lines indicate negative correlations. The thickness of each
576 line indicates the strength of the correlation ($|r| = 0.4 - 1$). The different colors in the names of the chemicals
577 correspond to the annotation levels of Schymanski et al.¹⁹ showing confidence in annotation. Level 1 are
578 compounds that have been confirmed with analytical standards, level 2 are compounds that have been tentatively
579 identified with MS/MS spectra matching and level 3 are compounds for which we have a definitive formula and
580 some diagnostic evidence based on our annotation algorithm described in materials and methods.

581

582 The maternal and cord networks (Fig. S9 and S10) showed great overlap with most chemical compounds
583 appearing in both networks and exhibiting similar relationships. Due to the complexity of the generated networks
584 (Fig. S9 and S10), we extracted some example subnetworks (Fig. 5 and 6) that illustrated correlations between

585 endogenous and exogenous compounds. The strongest association we observed between an endogenous and an
586 exogenous compound in both the maternal and cord networks was between ubiquinone q10 and Asarone ($r = 0.82$
587 in maternal network and $r = 0.80$ in cord network). We also observed two cyclic volatile methylsiloxanes (cVMS)
588 (octamethylcyclotetrasiloxane; D4 and decamethylcyclotetrasiloxane; D5) that correlated strongly with each other
589 ($r = 0.77$ in maternal network and $r = 0.81$ in cord network). In addition, in the maternal samples, D5 correlated
590 with benzaldehyde ($r = 0.41$), while in the cord samples, D4 and D5 correlated with silane
591 trimethyl(octadecyloxy)-, ($r = 0.41$ and 0.41) which in turn correlated with progesterone ($r = 0.55$) and ubiquinone
592 ($r = 0.45$). Finally, three perfluoroalkyl acids PFAAs: perfluorononanoic acid (PFNA), perfluorodecanoic acid
593 (PFDA) and perfluoroundecanoic acid (PFUnDA) correlated strongly with each other (r values in maternal: 0.66-
594 0.74, r values in cord: 0.64-0.72) while 2 perfluorinated sulfonic acids (PFSA; perfluorohexanesulfonic acid,
595 perfluorooctanesulfonic acid) formed their own group. Both groups of chemicals are poly/perfluoroalkyl
596 substances (PFAS), a group of chemicals that has recently come under scrutiny due to their persistence,
597 bioaccumulation potential and toxicity. The group of PFAA, in both networks, showed to correlate with certain
598 fatty acids, such as stearic acid and 4-oxopentanoic acid ($r = 0.4$ - 0.5) (Fig. 5 and 6).

599 4. Discussion

600 Our chemical analysis of the maternal and blood samples with HRMS and a non-target analysis workflow
601 provided important insights in the prenatal exposome, exposures to environmental pollutants, and their potential
602 role in the development of human disease. To our knowledge, this is the largest dataset of the exposome of
603 maternal and fetal exposures. We confirmed 19 with analytical standards (level 1), tentatively identified 73
604 compounds with MS/MS spectra matching (level 2) and annotated 98 features with our annotation algorithm
605 (level 3) described in the materials and methods (Supporting Spreadsheet 1: level 1-2 and level 3-4).

606 Our data analysis showed that when analyzing large sample sets with non-targeted analysis, batch effects
607 are substantial and they need to be adequately addressed before drawing any conclusions on the chemical,
608 biological, and epidemiological importance of that collected data. ComBat^{33,34} was able to remove batch effects
609 for HRMS data for exposomics and metabolomics analyses.

610 Maternal and cord samples showed similarities in chemical feature enrichment (Fig. 3), but also important
611 differences (Fig. 4) that allowed for these two groups to be classified as two distinct clusters (Fig. 4). Our
612 similarity network analyses also showed that matched maternal and cord samples are more similar in terms of
613 chemical feature enrichment compared to other maternal samples. These observations have important implications
614 when studying the partitioning of chemical compounds between maternal and cord samples and when studying
615 which chemicals show a stronger potential to cross the placenta and accumulate in the fetus. Previous studies have
616 reported on the partitioning between maternal and cord blood,⁵³⁻⁵⁶ however, the mechanism by which certain
617 chemicals cross the placenta more readily than others requires further investigation. One interesting example of
618 chemicals from our dataset that showed preferential partitioning for the maternal side were the five PFAS we
619 detected. The log R_{CM} of the five PFAS ranged from -0.037 to -0.22 (Supporting Spreadsheet 1 and Fig S5 B; left
620 tail of the distribution) indicating that the transfer of these chemicals to the fetus is to some degree inhibited by
621 the placenta. This finding is in good agreement with previous biomonitoring studies where they examined the
622 transplacental transfer of PFAS.^{57,58} Due to their strong affinity for proteins, PFAS, bind to the proteins in the
623 placenta and they are to some extent inhibited from reaching the fetus.^{57,58}

624 We observed a significant positive association between R_{CM} and E, and a significant negative association
625 between R_{CM} and K_{OW} indicating that R_{CM} is influenced by these two physicochemical properties. As E represents
626 the ability of a chemical to engage in London dispersion forces and dipole-induced dipole interactions, its positive
627 association with R_{CM} suggests that organic chemicals where large parts of the molecule are composed of C and H
628 without highly electronegative atoms (e.g., Cl) are more likely to partition preferably to cord blood. The negative
629 association of R_{CM} and K_{OW} suggests that hydrophobic molecules are likely to partition to maternal blood. This
630 observation is in agreement with previous studies showing a negative correlation between R_{CM} and K_{OW} .³⁶ We
631 observed a borderline significant relationship between R_{CM} for gestational age (0.07) (Fig. S6 C). Furthermore,
632 when we grouped the R_{CM} values by gestational age group, we observed a slightly higher median R_{CM} for preterm
633 birth samples compared to full term and late term (Fig. S6 E) indicating a higher overall transfer to the fetus in
634 preterm birth. However, this also appears to depend on the chemicals and their physicochemical properties. In an
635 earlier study on the transplacental transfer of PFAS Li et al.⁴¹ noted the reverse trend, namely, that transfer of

636 PFAS was higher in full term compared to preterm birth samples. We observed a slightly elevated median for
637 overall R_{CM} values in samples from patients with gestational diabetes. This finding, although, statistically not
638 significant, is in agreement with the study of Eryasa et al.⁴² that observed higher transplacental transfer in mothers
639 with gestational diabetes. These observations are in agreement with the thermodynamic understanding in
640 environmental chemistry that the behavior of chemicals is influenced by the chemicals' physicochemical
641 properties and by the properties of their environment.⁵⁹

642 We observed a weak but significant negative association between R_{CM} and RT (Fig. S5 D). As RT is a
643 function of the chemicals' hydrophobicity (K_{OW}), with more hydrophobic chemicals exhibiting longer RTs (Fig.
644 S6 H), its relationship with the R_{CM} indicates that more hydrophobic chemicals would show a preference to
645 partition more to the maternal blood compared to cord blood. This finding suggests that RT could be used as a
646 criterion for prioritizing chemical features for identification in maternal/cord blood studies and could potentially
647 also be used in prioritization of chemicals for toxicity testing. Finally, considering that K_{OW} can vary significantly
648 between structural isomers/isobaric features, the strong association we observed between $\log K_{OW}$ and RT ($r=0.79$,
649 $p=6.9e-33$) gives an extra degree of confidence for our annotations of the level 1, 2 and 3 chemicals. If these
650 annotations contained substantial errors one would expect to see greater variability in the data points for $\log K_{OW}$
651 and RT.

652 Our analysis of the associations between exogenous and endogenous exposures has provided a means to
653 uncover chemicals potentially important to biological pathways. Such findings are particularly useful because
654 they can be used to inform toxicological laboratory experiments to study the underlying molecular mechanisms.
655 We observed thousands of significant relationships between exogenous and endogenous chemical features,
656 hundreds of which showed an absolute $r > 0.5$. Many of these associations can be challenging to interpret in terms
657 of molecular mechanisms. Thus, we focused our discussion on associations that were both strong in terms of
658 correlation coefficient but also relatively easily interpretable.

659 The strongest association we observed between an endogenous and an exogenous compound in both the
660 maternal and the cord networks was that of ubiquinone q10 and Asarone. Ubiquinone q10 occurs naturally in the
661 human body in an oxidized (ubiquinone) and a reduced form (ubiquinol).⁶⁰ Ubiquinone acts as an electron and

662 proton carrier in mitochondrial electron transport connected to ATP synthesis. Ubiquinol acts as an antioxidant
663 inhibiting lipid peroxidation, protecting mitochondrial inner-membrane proteins and protecting DNA damage due
664 to oxidation.⁶⁰ Asarone is a chemical compound that occurs naturally in some plants, such as *Acorus calamus* and
665 it is used as a pesticide and as an essential oil in perfumes and in alcoholic beverages.⁶¹ Asarone is a carcinogenic
666 compound whose epoxide metabolite of is suspected of causing DNA damage.⁶² Based on the strong association
667 we observed for these two compounds, we hypothesize that exposure to Asarone may trigger the upregulation of
668 ubiquinone and ubiquinol. Despite its industrial applications, Asarone appeared to not be registered as a high
669 production volume chemical and it was not included in the Chemical Data Reporting database (CDR) under the
670 Toxic Substances Control Act (TSCA)⁶³. This raises some concerns about the regulation of Asarone and similar
671 toxic compounds that may have natural sources but are used in industrial applications.

672 Another group of exogenous chemicals that showed an interesting and pattern were three PFAS (PFNA,
673 PFDA and PFUnA) that positively correlated strongly ($r = 0.4-0.5$) with endogenous fatty acids (Fig 5 and 6)
674 indicating a potential interference with fatty acid metabolism. PFAS have been shown to interfere with fatty acid
675 metabolism in *in vitro* toxicological studies by binding to fatty acid binding proteins.^{64,65} Binding of PFAS to fatty
676 acid binding proteins could reduce the available binding sites for endogenous fatty acids resulting in higher
677 concentrations of fatty acids. This could explain the observed positive correlations between the three PFAS and
678 endogenous fatty acids in our study. Similar associations between PFAS and fatty acids have been reported in
679 previous metabolome/exposome studies^{66,67}, however, not for the exact same panel of PFAS and fatty acid
680 compounds and not through an NTA workflow. Currently there are about 10,000 PFAS registered on EPA's
681 Chemistry Dashboard, many of which do not have data on their toxicity potential in humans. Toxicological and
682 epidemiological studies have shown that exposure to certain PFAS is associated with altered liver function^{68,69},
683 increased risk for preterm birth, low birth weight⁷⁰, and lower bone mineral density⁷¹. Our study corroborates the
684 need for further experimental and modeling studies to assess the potential of the ever-increasing chemical library
685 of PFAS and study how they interfere with human metabolism. High-throughput protein binding studies would
686 help to elucidate some of these effects and help prioritize PFAS for biomonitoring and policy action.

687 Another group of chemicals that showed an interesting pattern were two cyclic volatile methylsiloxanes
688 (cVMS), octamethylcyclotetrasiloxane (D4) and decamethylcyclopentasiloxane (D5). cVMS are organosilicon
689 chemicals that are primarily used as carriers in personal care products, such as deodorants, and as intermediates in
690 the production of silicone polymers. Their strong positive correlation indicates a common source of exposure,
691 most likely due to use of personal care products. Their ubiquitous presence in personal care products makes it
692 very likely that these chemicals are from such applications. However, also because of their ubiquitous presence in
693 silicone polymers, there is a chance that these chemicals could be a result of contamination from inside the
694 analytical instrument. There is also a possibility that these chemicals could be also coming from personal care
695 products by people working in the lab, however, the physicochemical properties of D4 and D5, specifically their
696 equilibrium partition ratio between octanol and air (K_{OA}), indicates that partitioning from the air to an organic
697 solvent is very unlikely. D4 has a $\log K_{OA}$ of 4.97 and D5 has $\log K_{OA}$ of 3.94,²⁰ which indicate a strong
698 preference for the molecules to exist in the gas phase compared to other chemicals, such as polychlorobiphenyl
699 180 (PCB 180) which has a $\log K_{OA}$ of 9.94 and a much stronger preference to partition to octanol. Finally, all the
700 abundances in our data set were blank corrected which should minimize the potential of contamination. In the
701 maternal samples, D5 correlated with benzaldehyde which is a compound that occurs naturally in plants and in the
702 human body, and it is used as an additive in foods and personal care products.⁷² The correlation with D5 indicates
703 a common source of exposure through personal care products. In the cord samples, D4 and D5 correlated with
704 silane trimethyl(octadecyloxy)-, which in turn correlated with progesterone and ubiquinone. Silane
705 trimethyl(octadecyloxy)- is an organosilicon compound used in personal care products⁷³ and its correlation with
706 D4 and D5 makes good sense given the applications of these chemicals. The correlation of silane
707 trimethyl(octadecyloxy)- with progesterone and ubiquinone is somewhat concerning considering the wide use of
708 that chemical in personal care products.
709

710 5. Limitations and future considerations

711 Our study illustrates the importance of broad screening using NTA in order to characterize the exposome
712 and the mechanisms under which environmental exposures contribute to the development of human disease.
713 While NTA is a powerful tool in compound discovery, it also has its limitations as it is still early in its
714 development. One critical challenge with NTA is the small number of confirmed chemicals with analytical
715 standards, which is usually in the 10s, compared to the total number of detected features, which is usually in the
716 1000s.^{11,12,14,74} This obstacle restricts the ability of non-targeted analysis to assist in prioritizing chemicals for
717 biomonitoring and human exposure studies. Developing new computational tools for structure elucidation and
718 expanding *in silico* screening of databases for structures that correspond to detected formulas and prioritization of
719 hazardous chemicals can potentially help enhance our ability to utilize the potential of NTA.

720 A limitation of our study is that it uses only one analytical instrument, LC-QTOF/MS, which specializes
721 in the analysis and identification of polar and involatile compounds. As a result, the chemical features that we
722 detected are primarily from that physicochemical space. Complementing LC-QTOF/MS with gas chromatography
723 / mass spectrometry, especially high-resolution mass spectrometry and multidimensional techniques, could help
724 expand the spectrum of possible chemical features by including non-polar and volatile/semi-volatile chemicals.

725 Finally, our study focuses on the differences between maternal and cord blood as a surrogate for
726 understanding fetal exposure and adverse fetal health outcomes. However, adverse fetal health outcomes depend
727 not only on the amount of the chemical the fetus is exposed to, but also on the toxicity of the chemical. There is
728 thus a need to develop high-throughput toxicity screening models to screen for chemicals found in fetal blood.
729 Using NTA data to inform toxicity testing can provide unique insights in toxicology and environmental health and
730 assist in preventing of exposure to toxic chemicals.

731 In our future studies, we plan to conduct epidemiological analyses by further examining the correlations
732 of exogenous compounds with endogenous metabolites and examine the influence of covariates on these
733 associations. Furthermore, we plan to analyze additional samples from patients with adverse health outcomes to

734 enrich our dataset and investigate the role of endogenous and exogenous exposures to the development of adverse
735 health outcomes, such as gestational diabetes, preterm birth, birth weight, and preeclampsia, among others.

736

737 Data availability

738 All the datasets used are provided as supporting information. All the code is available on GitHub

739 (<https://github.com/dimitriabrahamsson/nontarget-maternalcord.git>)

740 All the MS and MS/MS files will be uploaded on the Metabolomics Workbench

741 (<https://www.metabolomicsworkbench.org/>) upon acceptance of the manuscript.

742 Acknowledgements

743 This study was funded by NIH/NIEHS grant numbers P30-ES030284, UG3OD023272, UH3OD023272,

744 P01ES022841, R01ES027051 and by the US EPA grant number RD83543301. We would like to thank the

745 clinical research coordinators for assisting in the collection of the samples and the data managers for their

746 assistance with the questionnaires and medical records. Finally, we would like to thank all the participants in the

747 Chemicals in Our Bodies cohort for their invaluable contribution.

748 Supporting Information

- 749 • Supporting Information: Figures S1-S10 and Tables S1 and S2
- 750 • Supporting Spreadsheet 0-database: The database of all chemical formulas and structures used in the
751 experimental analysis.
- 752 • Supporting Spreadsheet 1: Includes tables/spreadsheets referenced throughout the manuscript
- 753 • Supporting Spreadsheet 2-statistics: Includes correlation matrix data for endogenous and exogenous
754 compounds
- 755 • Supporting Spreadsheet 3-original data: Includes the original datasets before any processing

- 757 (1) Miller, G. W. *The Exposome*; Elsevier, 2014. <https://doi.org/10.1016/C2013-0-06870-3>.
- 758 (2) Wild, C. P. Complementing the Genome with an “Exposome”: The Outstanding Challenge of
759 Environmental Exposure Measurement in Molecular Epidemiology. *Cancer Epidemiol Biomarkers*
760 *Prev* **2005**, *14* (8), 1847–1850. <https://doi.org/10.1158/1055-9965.EPI-05-0456>.
- 761 (3) Rager, J. E.; Bangma, J.; Carberry, C.; Chao, A.; Grossman, J.; Lu, K.; Manuck, T. A.; Sobus, J.
762 R.; Szilagyi, J.; Fry, R. C. Review of the Environmental Prenatal Exposome and Its Relationship to
763 Maternal and Fetal Health. *Reproductive Toxicology* **2020**, *98*, 1–12.
764 <https://doi.org/10.1016/j.reprotox.2020.02.004>.
- 765 (4) Wang, A.; Padula, A.; Sirota, M.; Woodruff, T. J. Environmental Influences on Reproductive
766 Health: The Importance of Chemical Exposures. *Fertil. Steril.* **2016**, *106* (4), 905–929.
767 <https://doi.org/10.1016/j.fertnstert.2016.07.1076>.
- 768 (5) Gluckman, P. D.; Hanson, M. A. Living with the Past: Evolution, Development, and Patterns of
769 Disease. *Science* **2004**, *305* (5691), 1733–1736. <https://doi.org/10.1126/science.1095292>.
- 770 (6) Stillerman, K. P.; Mattison, D. R.; Giudice, L. C.; Woodruff, T. J. Environmental Exposures and
771 Adverse Pregnancy Outcomes: A Review of the Science. *Reprod Sci* **2008**, *15* (7), 631–650.
772 <https://doi.org/10.1177/1933719108322436>.
- 773 (7) US EPA, O. TSCA Chemical Substance Inventory <https://www.epa.gov/tsca-inventory> (accessed
774 Mar 18, 2020).
- 775 (8) US EPA, O. TSCA Inventory Notification (Active-Inactive) Rule [https://www.epa.gov/tsca-](https://www.epa.gov/tsca-inventory/tsca-inventory-notification-active-inactive-rule)
776 [inventory/tsca-inventory-notification-active-inactive-rule](https://www.epa.gov/tsca-inventory/tsca-inventory-notification-active-inactive-rule) (accessed Mar 18, 2020).
- 777 (9) Wang Aolin; Gerona Roy R.; Schwartz Jackie M.; Lin Thomas; Sirota Marina; Morello-Frosch
778 Rachel; Woodruff Tracey J. A Suspect Screening Method for Characterizing Multiple Chemical
779 Exposures among a Demographically Diverse Population of Pregnant Women in San Francisco.
780 *Environmental Health Perspectives* *126* (7), 077009. <https://doi.org/10.1289/EHP2920>.
- 781 (10) Moschet, C.; Anumol, T.; Lew, B. M.; Bennett, D. H.; Young, T. M. Household Dust as a
782 Repository of Chemical Accumulation: New Insights from a Comprehensive High-Resolution Mass
783 Spectrometric Study. *Environ. Sci. Technol.* **2018**, *52* (5), 2878–2887.
784 <https://doi.org/10.1021/acs.est.7b05767>.
- 785 (11) Newton, S. R.; McMahan, R. L.; Sobus, J. R.; Mansouri, K.; Williams, A. J.; McEachran, A. D.;
786 Strynar, M. J. Suspect Screening and Non-Targeted Analysis of Drinking Water Using Point-of-
787 Use Filters. *Environmental Pollution* **2018**, *234*, 297–306.
788 <https://doi.org/10.1016/j.envpol.2017.11.033>.
- 789 (12) Rager, J. E.; Strynar, M. J.; Liang, S.; McMahan, R. L.; Richard, A. M.; Grulke, C. M.; Wambaugh,
790 J. F.; Isaacs, K. K.; Judson, R.; Williams, A. J.; Sobus, J. R. Linking High Resolution Mass
791 Spectrometry Data with Exposure and Toxicity Forecasts to Advance High-Throughput
792 Environmental Monitoring. *Environment International* **2016**, *88*, 269–280.
793 <https://doi.org/10.1016/j.envint.2015.12.008>.
- 794 (13) Phillips, K. A.; Yau, A.; Favela, K. A.; Isaacs, K. K.; McEachran, A.; Grulke, C.; Richard, A. M.;
795 Williams, A. J.; Sobus, J. R.; Thomas, R. S.; Wambaugh, J. F. Suspect Screening Analysis of
796 Chemicals in Consumer Products. *Environ. Sci. Technol.* **2018**, *52* (5), 3125–3135.
797 <https://doi.org/10.1021/acs.est.7b04781>.
- 798 (14) Wang, A.; Abrahamsson, D. P.; Jiang, T.; Wang, M.; Morello-Frosch, R.; Park, J.-S.; Sirota, M.;
799 Woodruff, T. J. Suspect Screening, Prioritization, and Confirmation of Environmental Chemicals in
800 Maternal-Newborn Pairs from San Francisco. *Environ. Sci. Technol.* **2021**.
801 <https://doi.org/10.1021/acs.est.0c05984>.

- 802 (15) Schultes, L.; van Noordenburg, C.; Spaan, K. M.; Plassmann, M. M.; Simon, M.; Roos, A.;
803 Benskin, J. P. High Concentrations of Unidentified Extractable Organofluorine Observed in
804 Blubber from a Greenland Killer Whale (*Orcinus Orca*). *Environ. Sci. Technol. Lett.* **2020**, *7* (12),
805 909–915. <https://doi.org/10.1021/acs.estlett.0c00661>.
- 806 (16) Sobus, J. R.; Grossman, J. N.; Chao, A.; Singh, R.; Williams, A. J.; Grulke, C. M.; Richard, A. M.;
807 Newton, S. R.; McEachran, A. D.; Ulrich, E. M. Using Prepared Mixtures of ToxCast Chemicals to
808 Evaluate Non-Targeted Analysis (NTA) Method Performance. *Anal Bioanal Chem* **2019**, *411* (4),
809 835–851. <https://doi.org/10.1007/s00216-018-1526-4>.
- 810 (17) Lai, A.; Singh, R. R.; Kovalova, L.; Jaeggi, O.; Kondić, T.; Schymanski, E. L. Retrospective Non-
811 Target Analysis to Support Regulatory Water Monitoring: From Masses of Interest to
812 Recommendations via in Silico Workflows. *Environmental Sciences Europe* **2021**, *33* (1), 43.
813 <https://doi.org/10.1186/s12302-021-00475-1>.
- 814 (18) Singh, R. R.; Chao, A.; Phillips, K. A.; Xia, X. R.; Shea, D.; Sobus, J. R.; Schymanski, E. L.; Ulrich,
815 E. M. Expanded Coverage of Non-Targeted LC-HRMS Using Atmospheric Pressure Chemical
816 Ionization: A Case Study with ENTACT Mixtures. *Anal Bioanal Chem* **2020**, *412* (20), 4931–4939.
817 <https://doi.org/10.1007/s00216-020-02716-3>.
- 818 (19) Schymanski, E. L.; Jeon, J.; Gulde, R.; Fenner, K.; Ruff, M.; Singer, H. P.; Hollender, J. Identifying
819 Small Molecules via High Resolution Mass Spectrometry: Communicating Confidence. *Environ.*
820 *Sci. Technol.* **2014**, *48* (4), 2097–2098. <https://doi.org/10.1021/es5002105>.
- 821 (20) U.S. Environmental Protection Agency. Chemistry Dashboard <https://comptox.epa.gov/dashboard/>
822 (accessed Mar 9, 2021).
- 823 (21) Horai, H.; Arita, M.; Kanaya, S.; Nihei, Y.; Ikeda, T.; Suwa, K.; Ojima, Y.; Tanaka, K.; Tanaka, S.;
824 Aoshima, K.; Oda, Y.; Kakazu, Y.; Kusano, M.; Tohge, T.; Matsuda, F.; Sawada, Y.; Hirai, M. Y.;
825 Nakanishi, H.; Ikeda, K.; Akimoto, N.; Maoka, T.; Takahashi, H.; Ara, T.; Sakurai, N.; Suzuki, H.;
826 Shibata, D.; Neumann, S.; Iida, T.; Tanaka, K.; Funatsu, K.; Matsuura, F.; Soga, T.; Taguchi, R.;
827 Saito, K.; Nishioka, T. MassBank: A Public Repository for Sharing Mass Spectral Data for Life
828 Sciences. *Journal of Mass Spectrometry* **2010**, *45* (7), 703–714. <https://doi.org/10.1002/jms.1777>.
- 829 (22) MassBank I MassBank Europe Mass Spectral DataBase <https://massbank.eu/MassBank/>
830 (accessed Jan 20, 2021).
- 831 (23) MassBank of North America <https://mona.fiehnlab.ucdavis.edu/> (accessed Jan 20, 2021).
- 832 (24) Wishart, D. S.; Feunang, Y. D.; Marcu, A.; Guo, A. C.; Liang, K.; Vázquez-Fresno, R.; Sajed, T.;
833 Johnson, D.; Li, C.; Karu, N.; Sayeeda, Z.; Lo, E.; Assempour, N.; Berjanskii, M.; Singhal, S.;
834 Arndt, D.; Liang, Y.; Badran, H.; Grant, J.; Serra-Cayuela, A.; Liu, Y.; Mandal, R.; Neveu, V.; Pon,
835 A.; Knox, C.; Wilson, M.; Manach, C.; Scalbert, A. HMDB 4.0: The Human Metabolome Database
836 for 2018. *Nucleic acids research* **2018**, *46* (D1), D608–D617. <https://doi.org/10.1093/nar/gkx1089>.
- 837 (25) Human Metabolome Database <http://www.hmdb.ca/> (accessed Feb 19, 2020).
- 838 (26) mzCloud - Advanced Mass Spectral Database <https://www.mzcloud.org/>.
- 839 (27) Allen, F.; Pon, A.; Wilson, M.; Greiner, R.; Wishart, D. CFM-ID: A Web Server for Annotation,
840 Spectrum Prediction and Metabolite Identification from Tandem Mass Spectra. *Nucleic Acids*
841 *Research* **2014**, *42* (W1), W94–W99. <https://doi.org/10.1093/nar/gku436>.
- 842 (28) Allen, F.; Greiner, R.; Wishart, D. Competitive Fragmentation Modeling of ESI-MS/MS Spectra for
843 Putative Metabolite Identification. *Metabolomics* **2015**, *11* (1), 98–110.
844 <https://doi.org/10.1007/s11306-014-0676-4>.
- 845 (29) CompMS I MS-DIAL <http://prime.psc.riken.jp/compms/msdial/main.html> (accessed Nov 13, 2020).
- 846 (30) WikiPathways - WikiPathways <https://www.wikipathways.org/index.php/WikiPathways> (accessed
847 Sep 23, 2020).
- 848 (31) Wikipedia <https://www.wikipedia.org/> (accessed Sep 23, 2020).

- 849 (32) Anna, S.; Sofia, B.; Christina, R.; Magnus, B. The Dilemma in Prioritizing Chemicals for
850 Environmental Analysis: Known versus Unknown Hazards. *Environ. Sci.: Processes Impacts*
851 **2016**, *18* (8), 1042–1049. <https://doi.org/10.1039/C6EM00163G>.
- 852 (33) GitHub - brentp/combat.py: python / numpy / pandas / patsy version of ComBat for removing batch
853 effects. <https://github.com/brentp/combat.py> (accessed Apr 3, 2020).
- 854 (34) Adjusting batch effects in microarray expression data using empirical Bayes methods I
855 Biostatistics I Oxford Academic <https://academic.oup.com/biostatistics/article/8/1/118/252073>
856 (accessed Apr 3, 2020).
- 857 (35) Software for Complex Networks — NetworkX 2.5 documentation
858 <https://networkx.github.io/documentation/stable/index.html> (accessed Sep 11, 2020).
- 859 (36) Lancz, K.; Murínová, L.; Patayová, H.; Drobná, B.; Wimmerová, S.; Šovčíková, E.; Kováč, J.;
860 Farkašová, D.; Hertz-Picciotto, I.; Jusko, T. A.; Trnovec, T. Ratio of Cord to Maternal Serum PCB
861 Concentrations in Relation to Their Congener-Specific Physicochemical Properties. *International*
862 *Journal of Hygiene and Environmental Health* **2015**, *218* (1), 91–98.
863 <https://doi.org/10.1016/j.ijheh.2014.08.003>.
- 864 (37) Aylward, L. L.; Hays, S. M.; Kirman, C. R.; Marchitti, S. A.; Kenneke, J. F.; English, C.; Mattison,
865 D. R.; Becker, R. A. Relationships of Chemical Concentrations in Maternal and Cord Blood: A
866 Review of Available Data. *Journal of toxicology and environmental health. Part B, Critical reviews*
867 **2014**, *17* (3), 175–203. <https://doi.org/10.1080/10937404.2014.884956>.
- 868 (38) Morello-Frosch, R.; Cushing, L. J.; Jesdale, B. M.; Schwartz, J. M.; Guo, W.; Guo, T.; Wang, M.;
869 Harwani, S.; Petropoulou, S.-S. E.; Duong, W.; Park, J. J.; Petreas, M. X.; Gajek, R.; Alvaran, J.;
870 She, J.; Dobraca, D.; Das, R.; Woodruff, T. J. Environmental Chemicals in an Urban Population of
871 Pregnant Women and Their Newborns from San Francisco. *Environmental Science & Technology*
872 **2016**, *50* (22), 12464–12472. <https://doi.org/10.1021/acs.est.6b03492>.
- 873 (39) Li, J.; Sun, X.; Xu, J.; Tan, H.; Zeng, E. Y.; Chen, D. Transplacental Transfer of Environmental
874 Chemicals: Roles of Molecular Descriptors and Placental Transporters. *Environ. Sci. Technol.*
875 **2021**, *55* (1), 519–528. <https://doi.org/10.1021/acs.est.0c06778>.
- 876 (40) Jeong, Y.; Lee, S.; Kim, S.; Park, J.; Kim, H.-J.; Choi, G.; Choi, S.; Kim, S.; Kim, S. Y.; Kim, S.;
877 Choi, K.; Moon, H.-B. Placental Transfer of Persistent Organic Pollutants and Feasibility Using the
878 Placenta as a Non-Invasive Biomonitoring Matrix. *Science of The Total Environment* **2018**, *612*,
879 1498–1505. <https://doi.org/10.1016/j.scitotenv.2017.07.054>.
- 880 (41) Li, J.; Cai, D.; Chu, C.; Li, Q.; Zhou, Y.; Hu, L.; Yang, B.; Dong, G.; Zeng, X.; Chen, D.
881 Transplacental Transfer of Per- and Polyfluoroalkyl Substances (PFASs): Differences between
882 Preterm and Full-Term Deliveries and Associations with Placental Transporter mRNA Expression.
883 *Environ. Sci. Technol.* **2020**, *54* (8), 5062–5070. <https://doi.org/10.1021/acs.est.0c00829>.
- 884 (42) Eryasa, B.; Grandjean, P.; Nielsen, F.; Valvi, D.; Zmirou-Navier, D.; Sunderland, E.; Weihe, P.;
885 Oulhote, Y. Physico-Chemical Properties and Gestational Diabetes Predict Transplacental
886 Transfer and Partitioning of Perfluoroalkyl Substances. *Environment International* **2019**, *130*,
887 104874. <https://doi.org/10.1016/j.envint.2019.05.068>.
- 888 (43) Abraham, M. H. Scales of Solute Hydrogen-Bonding: Their Construction and Application to
889 Physicochemical and Biochemical Processes. *Chem. Soc. Rev.* **1993**, *22* (2), 73–83.
890 <https://doi.org/10.1039/CS9932200073>.
- 891 (44) Abraham, M. H.; Ibrahim, A.; Zissimos, A. M. Determination of Sets of Solute Descriptors from
892 Chromatographic Measurements. *Journal of Chromatography A* **2004**, *1037* (1), 29–47.
893 <https://doi.org/10.1016/j.chroma.2003.12.004>.
- 894 (45) Abraham, M. H.; Smith, R. E.; Luchtefeld, R.; Boorem, A. J.; Luo, R.; Acree, W. E. Prediction of
895 Solubility of Drugs and Other Compounds in Organic Solvents. *Journal of Pharmaceutical*
896 *Sciences* **2010**, *99* (3), 1500–1515. <https://doi.org/10.1002/jps.21922>.

- 897 (46) Ulrich, N.; E., S.; Brown, T. N.; Watanabe, N.; Bronner, G.; Abraham, M. H.; Goss, K. U.
898 UFZ-LSER Database v 3.2 [Internet]. **2017**.
- 899 (47) Ideker, T.; Ozier, O.; Schwikowski, B.; Siegel, A. F. Discovering Regulatory and Signalling Circuits
900 in Molecular Interaction Networks. *Bioinformatics* **2002**, *18* (suppl_1), S233–S240.
901 https://doi.org/10.1093/bioinformatics/18.suppl_1.S233.
- 902 (48) Schramm, S.-J.; Jayaswal, V.; Goel, A.; Li, S. S.; Yang, Y. H.; Mann, G. J.; Wilkins, M. R.
903 Molecular Interaction Networks for the Analysis of Human Disease: Utility, Limitations, and
904 Considerations. *PROTEOMICS* **2013**, *13* (23–24), 3393–3405.
905 <https://doi.org/10.1002/pmic.201200570>.
- 906 (49) Winterbach, W.; Mieghem, P. V.; Reinders, M.; Wang, H.; Ridder, D. de. Topology of Molecular
907 Interaction Networks. *BMC Systems Biology* **2013**, *7* (1), 90. [https://doi.org/10.1186/1752-0509-7-](https://doi.org/10.1186/1752-0509-7-90)
908 [90](https://doi.org/10.1186/1752-0509-7-90).
- 909 (50) Interactome. *Wikipedia*; 2021.
- 910 (51) Cytoscape: An Open Source Platform for Complex Network Analysis and Visualization
911 <https://cytoscape.org/> (accessed Sep 24, 2020).
- 912 (52) MetScape 3 <http://metscape.ncibi.org/> (accessed Sep 24, 2020).
- 913 (53) Kato, K.; Wong, L.-Y.; Chen, A.; Dunbar, C.; Webster, G. M.; Lanphear, B. P.; Calafat, A. M.
914 Changes in Serum Concentrations of Maternal Poly- and Perfluoroalkyl Substances over the
915 Course of Pregnancy and Predictors of Exposure in a Multiethnic Cohort of Cincinnati, Ohio
916 Pregnant Women during 2003–2006. *Environ. Sci. Technol.* **2014**, *48* (16), 9600–9608.
917 <https://doi.org/10.1021/es501811k>.
- 918 (54) Pan, Y.; Deng, M.; Li, J.; Du, B.; Lan, S.; Liang, X.; Zeng, L. Occurrence and Maternal Transfer of
919 Multiple Bisphenols, Including an Emerging Derivative with Unexpectedly High Concentrations, in
920 the Human Maternal–Fetal–Placental Unit. *Environ. Sci. Technol.* **2020**, *54* (6), 3476–3486.
921 <https://doi.org/10.1021/acs.est.0c00206>.
- 922 (55) Chen, F.; Yin, S.; Kelly, B. C.; Liu, W. Isomer-Specific Transplacental Transfer of Perfluoroalkyl
923 Acids: Results from a Survey of Paired Maternal, Cord Sera, and Placentas. *Environ. Sci.*
924 *Technol.* **2017**, *51* (10), 5756–5763. <https://doi.org/10.1021/acs.est.7b00268>.
- 925 (56) Chen, A.; Park, J.-S.; Linderholm, L.; Rhee, A.; Petreas, M.; DeFranco, E. A.; Dietrich, K. N.; Ho,
926 S. Hydroxylated Polybrominated Diphenyl Ethers in Paired Maternal and Cord Sera. *Environ. Sci.*
927 *Technol.* **2013**, *47* (8), 3902–3908. <https://doi.org/10.1021/es3046839>.
- 928 (57) Mamsen, L. S.; Björvang, R. D.; Mucs, D.; Vinnars, M.-T.; Papadogiannakis, N.; Lindh, C. H.;
929 Andersen, C. Y.; Damdimopoulou, P. Concentrations of Perfluoroalkyl Substances (PFASs) in
930 Human Embryonic and Fetal Organs from First, Second, and Third Trimester Pregnancies.
931 *Environment International* **2019**, *124*, 482–492. <https://doi.org/10.1016/j.envint.2019.01.010>.
- 932 (58) Mamsen, L. S.; Jönsson, B. A. G.; Lindh, C. H.; Olesen, R. H.; Larsen, A.; Ernst, E.; Kelsey, T. W.;
933 Andersen, C. Y. Concentration of Perfluorinated Compounds and Cotinine in Human Foetal
934 Organs, Placenta, and Maternal Plasma. *Science of The Total Environment* **2017**, *596–597*, 97–
935 105. <https://doi.org/10.1016/j.scitotenv.2017.04.058>.
- 936 (59) Environmental Organic Chemistry, 3rd Edition | Wiley [https://www.wiley.com/en-](https://www.wiley.com/en-us/Environmental+Organic+Chemistry%2C+3rd+Edition-p-9781118767238)
937 [us/Environmental+Organic+Chemistry%2C+3rd+Edition-p-9781118767238](https://www.wiley.com/en-us/Environmental+Organic+Chemistry%2C+3rd+Edition-p-9781118767238) (accessed May 4,
938 2021).
- 939 (60) Ernster, L.; Dallner, G. Biochemical, Physiological and Medical Aspects of Ubiquinone Function.
940 *Biochimica et Biophysica Acta (BBA) - Molecular Basis of Disease* **1995**, *1271* (1), 195–204.
941 [https://doi.org/10.1016/0925-4439\(95\)00028-3](https://doi.org/10.1016/0925-4439(95)00028-3).
- 942 (61) PubChem. PubChem <https://pubchem.ncbi.nlm.nih.gov/> (accessed Aug 25, 2020).
- 943 (62) Cartus, A. T.; Schrenk, D. Metabolism of the Carcinogen Alpha-Asarone in Liver Microsomes.
944 *Food and Chemical Toxicology* **2016**, *87*, 103–112. <https://doi.org/10.1016/j.fct.2015.11.021>.

- 945 (63) US EPA, O. Chemical Data Reporting under the Toxic Substances Control Act
946 <https://www.epa.gov/chemical-data-reporting> (accessed May 4, 2021).
- 947 (64) Sheng, N.; Cui, R.; Wang, J.; Guo, Y.; Wang, J.; Dai, J. Cytotoxicity of Novel Fluorinated
948 Alternatives to Long-Chain Perfluoroalkyl Substances to Human Liver Cell Line and Their Binding
949 Capacity to Human Liver Fatty Acid Binding Protein. *Arch Toxicol* **2018**, *92* (1), 359–369.
950 <https://doi.org/10.1007/s00204-017-2055-1>.
- 951 (65) Zhang, L.; Ren, X.-M.; Guo, L.-H. Structure-Based Investigation on the Interaction of
952 Perfluorinated Compounds with Human Liver Fatty Acid Binding Protein. *Environ. Sci. Technol.*
953 **2013**, *47* (19), 11293–11301. <https://doi.org/10.1021/es4026722>.
- 954 (66) Alderete, T. L.; Jin, R.; Walker, D. I.; Valvi, D.; Chen, Z.; Jones, D. P.; Peng, C.; Gilliland, F. D.;
955 Berhane, K.; Conti, D. V.; Goran, M. I.; Chatzi, L. Perfluoroalkyl Substances, Metabolomic
956 Profiling, and Alterations in Glucose Homeostasis among Overweight and Obese Hispanic
957 Children: A Proof-of-Concept Analysis. *Environment International* **2019**, *126*, 445–453.
958 <https://doi.org/10.1016/j.envint.2019.02.047>.
- 959 (67) Chen, Z.; Yang, T.; Walker, D. I.; Thomas, D. C.; Qiu, C.; Chatzi, L.; Alderete, T. L.; Kim, J. S.;
960 Conti, D. V.; Breton, C. V.; Liang, D.; Hauser, E. R.; Jones, D. P.; Gilliland, F. D. Dysregulated
961 Lipid and Fatty Acid Metabolism Link Perfluoroalkyl Substances Exposure and Impaired Glucose
962 Metabolism in Young Adults. *Environment International* **2020**, *145*, 106091.
963 <https://doi.org/10.1016/j.envint.2020.106091>.
- 964 (68) Bassler, J.; Ducatman, A.; Elliott, M.; Wen, S.; Wahlang, B.; Barnett, J.; Cave, M. C.
965 Environmental Perfluoroalkyl Acid Exposures Are Associated with Liver Disease Characterized by
966 Apoptosis and Altered Serum Adipocytokines. *Environmental Pollution* **2019**, *247*, 1055–1063.
967 <https://doi.org/10.1016/j.envpol.2019.01.064>.
- 968 (69) Salihovic, S.; Stubleski, J.; Kärrman, A.; Larsson, A.; Fall, T.; Lind, L.; Lind, P. M. Changes in
969 Markers of Liver Function in Relation to Changes in Perfluoroalkyl Substances - A Longitudinal
970 Study. *Environment International* **2018**, *117*, 196–203.
971 <https://doi.org/10.1016/j.envint.2018.04.052>.
- 972 (70) Li, M.; Zeng, X.-W.; Qian, Z. (Min); Vaughn, M. G.; Sauv e, S.; Paul, G.; Lin, S.; Lu, L.; Hu, L.-W.;
973 Yang, B.-Y.; Zhou, Y.; Qin, X.-D.; Xu, S.-L.; Bao, W.-W.; Zhang, Y.-Z.; Yuan, P.; Wang, J.; Zhang,
974 C.; Tian, Y.-P.; Nian, M.; Xiao, X.; Fu, C.; Dong, G.-H. Isomers of Perfluorooctanesulfonate
975 (PFOS) in Cord Serum and Birth Outcomes in China: Guangzhou Birth Cohort Study. *Environment*
976 *International* **2017**, *102*, 1–8. <https://doi.org/10.1016/j.envint.2017.03.006>.
- 977 (71) Khalil Naila; Chen Aimin; Lee Miryoung; Czerwinski Stefan A.; Ebert James R.; DeWitt Jamie C.;
978 Kannan Kurunthachalam. Association of Perfluoroalkyl Substances, Bone Mineral Density, and
979 Osteoporosis in the U.S. Population in NHANES 2009–2010. *Environmental Health Perspectives*
980 **2016**, *124* (1), 81–87. <https://doi.org/10.1289/ehp.1307909>.
- 981 (72) PubChem. Benzaldehyde <https://pubchem.ncbi.nlm.nih.gov/compound/240> (accessed May 4,
982 2021).
- 983 (73) PubChem. Silane, trimethyl(octadecyloxy)- <https://pubchem.ncbi.nlm.nih.gov/compound/87778>
984 (accessed May 4, 2021).
- 985 (74) Wang Aolin; Gerona Roy R.; Schwartz Jackie M.; Lin Thomas; Sirota Marina; Morello-Frosch
986 Rachel; Woodruff Tracey J. A Suspect Screening Method for Characterizing Multiple Chemical
987 Exposures among a Demographically Diverse Population of Pregnant Women in San Francisco.
988 *Environmental Health Perspectives* *126* (7), 077009. <https://doi.org/10.1289/EHP2920>.
989